Measurements of semileptonic branching fractions of B mesons at the $\Upsilon(4S)$ resonance

S. Henderson, K. Kinoshita, F. Pipkin, M. Procario, M. Saulnier, R. Wilson, J. Wolinski, and D. Xiao
Harvard University, Cambridge, Massachusetts 02138

R. Ammar, P. Baringer, D. Coppage, R. Davis, P. Haas, M. Kelly, N. Kwak, Ha Lam, and S. Ro
University of Kansas, Lawrence, Kansas 66045

Y. Kubota, J.K. Nelson, D. Perticone, R. Poling, and S. Schrenk
University of Minnesota, Minneapolis, Minnesota 55455

G. Crawford, R. Fulton, T. Jensen, D.R. Johnson, H. Kagan, R. Kass, R. Malchow, F. Morrow, J. Whitmore, and P. Wilson
Ohio State University, Columbus, Ohio 43210

D. Bortoletto, D. Brown, J. Dominick, R.L. McIlwain, D.H. Miller, M. Modesitt, S.F. Schaffner, E.I. Shibata, and I.P.J. Shipsey
Purdue University, West Lafayette, Indiana 47907

M. Battle, H. Kroha, K. Sparks, E.H. Thorndike, and C.-H. Wang
University of Rochester, Rochester, New York 14627

M.S. Alam, I.J. Kim, W.C. Li, B. Nemati, V. Romero, C.R. Sun, P.-N. Wang, and M.M. Zoeller
State University of New York at Albany, Albany, New York 12222

M. Goldberg, T. Haupt, N. Horwitz, V. Jain, Rosemary Kennett, M.D. Mestayer, G.C. Moneti, Y. Rozen, P. Rubin, T. Skwarnicki, S. Stone, M. Thusalidas, W.-M. Yao, and G. Zhu
Syracuse University, Syracuse, New York 13244

A.V. Barnes, J. Bartelt, S.E. Csorna, and T. Letson
Vanderbilt University, Nashville, Tennessee 37235

J. Alexander, M. Artuso, C. Bebek, K. Berkelman, D. Besson, T. Browder, D.G. Cassel, E. Cheu, D.M. Coffman, J.W. DeWire,* P.S. Drell, R. Ehrlich, R.S. Galik, M. Garcia-Sciveres, B. Geiser, B. Gittelman, S.W. Gray, A.M. Halling, D.L. Hartill, B.K. Heltsley, K. Honscheid, J. Kandaswamy, N. Katayama, R. Kowalewski, D.L. Kreinick, J.D. Lewis, G.S. Ludwig, J. Masui, J. Mevissen, N.B. Mistry, S. Nandi, C.R. Ng, E. Nordberg, C. O'Grady, J.R. Patterson, D. Peterson, M. Pisharody, D. Riley, M. Sapper, M. Selen, A. Silverman, H. Worden, and M. Worris
Cornell University, Ithaca, New York 14853

A. J. Sadoff
Ithaca College, Ithaca, New York 14850

P. Avery, A. Freyberger, J. Rodriguez, and J. Yelton
University of Florida, Gainesville, Florida 32611

(CLEO Collaboration)

*Deceased.

(Received 8 July 1991)

We report new measurements of semileptonic branching fractions of B mesons produced at the $\Upsilon(4S)$ resonance determined by fitting the inclusive electron and muon momentum spectra to different theoretical models. Using $B(\bar{B} \to X\ell^-\bar{\nu})$ to denote the *average* of the semileptonic branching fractions for B decay to electrons and muons, we obtain $B(\bar{B} \to X\ell^-\bar{\nu}) = (10.5 \pm 0.2 \pm 0.4)\%$ using the refined free-quark model of Altarelli *et al.*, and $B(\bar{B} \to X\ell^-\bar{\nu}) = (11.2 \pm 0.3 \pm 0.4)\%$ using a modified version of the form-factor model of Isgur *et al.*, in which the $D^{**}\ell^-\bar{\nu}$ contribution is allowed to float in the fit. The average of these two results is $B(\bar{B} \to X\ell^-\bar{\nu}) = (10.8 \pm 0.2 \pm 0.4 \pm 0.4)\%$, where the errors are statistical, systematic uncertainties in the measurement, and systematic uncertainties associated with the theoretical models, respectively. Semileptonic branching fractions as low as this are difficult to accommodate in theoretical models where hadronic B-meson decays arise only from spectator diagrams. We use dilepton yields to limit the uncertainty in the semileptonic branching fraction due to the possible existence of non-$B\bar{B}$ decays of the $\Upsilon(4S)$. In addition, we tag neutral B mesons using the decays $\bar{B}^0 \to D^{*+}\pi^-$ and $\bar{B}^0 \to D^{*+}\ell^-\bar{\nu}$ to obtain the first direct measurement of semileptonic branching fractions for neutral B mesons; the average of the electron and muon results for neutral B mesons is $B(\bar{B}^0 \to X\ell^-\bar{\nu}) = (9.9 \pm 3.0 \pm 0.9)\%$.

PACS number(s): 13.20.Jf, 14.40.Jz

I. INTRODUCTION

In the most naive picture, dominance of spectator diagrams in heavy-quark decay implies that the lifetimes and semileptonic branching fractions [1] of hadrons containing a heavy quark should not depend on the kind or number of light quarks in the hadron [2]. (Diagrams for B-meson decay are illustrated in Fig. 1.) The large difference between the lifetimes for charged and neutral D mesons demonstrates that this naive picture is not correct for charm decay [3]. Various theoretical explanations include either nonspectator processes or the interference between internal and external spectator diagrams, illustrated in Fig. 2, which can occur when one of the light quarks from the W is identical to the spectator quark [4–7]. Because the b quark is heavier than the c quark, both nonspectator processes and interference are expected to be less important in B-meson decay [8]. Since semileptonic decays arise only from spectator diagrams in the standard model, they play a central part in elucidating the role of these diagrams in the weak decay of heavy quarks. In particular, they provide a means of measuring the Cabibbo-Kobayashi-Maskawa (CKM) matrix elements [9] $|V_{cb}|$ and $|V_{ub}|$ with less theoretical uncertainty than measurements based on hadronic decays of B mesons.

Theoretical predictions [10] of the semileptonic branching fraction for B-meson decay based on the spectator model are generally above 12%. One recent measurement [11] is consistent with this prediction, but a number of other measurements [12–15] suggest that the semileptonic branching fraction for B-meson decay is below 11%. A recent study [16] indicates that nonspectator processes such as W exchange may enhance the hadronic width enough to lower the theoretical estimate of the semileptonic branching fraction to as little as 10–11%.

In this paper we report new measurements of the semileptonic branching fractions of B mesons which were made with the CLEO detector at the Cornell Electron Storage Ring (CESR). Our B-meson [17] sample comes from $\Upsilon(4S) \to B\bar{B}$ events; in Sec. II we discuss the parameters to be measured in semileptonic B decay at the $\Upsilon(4S)$. After description of our $\Upsilon(4S)$ data sample in Sec. III, we present new measurements of the B-meson semileptonic branching fraction in Sec. IV. We include a new technique using dilepton events to measure the semileptonic branching fraction independently of the branching fraction for $\Upsilon(4S)$ decays to non-$B\bar{B}$ states. Section V describes measurements of the semileptonic branching fraction of the neutral B meson obtained

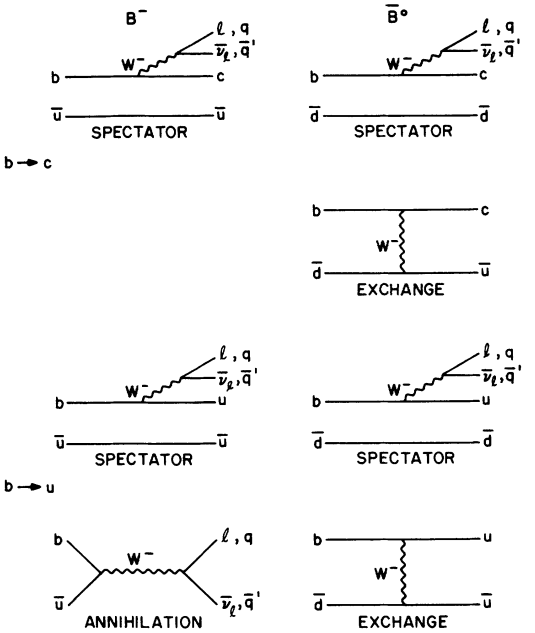

FIG. 1. The spectator, exchange, and annihilation diagrams for B^- and $\bar{B}^0$ decay. Note that semileptonic decay widths are completely dominated by the spectator diagrams because the exchange diagrams do not produce leptons and the annihilation diagram for B^- decay is strongly Cabibbo-suppressed since it involves a $b \to u$ transition. If the exchange contributions are important, the B^- and $\bar{B}^0$ lifetimes would be different, resulting in different semileptonic branching fractions for B^- and $\bar{B}^0$ decays.

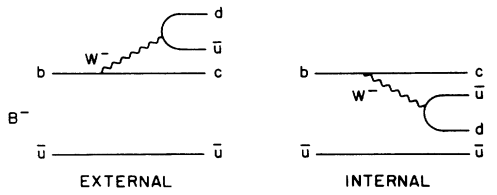

FIG. 2. External and internal spectator diagrams for B^- decay. In the external diagram, the quarks produced by the W^- decay hadronize separately from the spectator quark and the c quark from b-quark decay, while in the internal or "color-mixed" diagram the opposite is true. Since the quark-antiquark pairs involved in hadronization have identical flavor in the two diagrams, the diagrams can interfere.

using two methods to tag neutral B mesons. Conclusions are presented in Sec. VI.

II. PARAMETERS TO BE MEASURED

Five parameters are required to describe the inclusive lepton yields of B mesons from $\Upsilon(4S)$ decays: b_- and b_0, the semileptonic branching fractions of charged and neutral B mesons, respectively; f_- and f_0, the branching fractions of the $\Upsilon(4S)$ to charged and neutral B mesons, respectively; and r, the $B^0\bar{B}^0$ mixing parameter. Measurements of various lepton yields at the $\Upsilon(4S)$ yield measurements of different combinations of these parameters. Several ratios of these quantities are important:

$$\beta = \frac{b_-}{b_0}, \tag{1}$$

$$\phi = \frac{f_-}{f_0}, \tag{2}$$

$$\lambda = \frac{f_- b_-^2}{f_0 b_0^2}, \tag{3}$$

$$\mu = \frac{f_- b_-}{f_0 b_0}. \tag{4}$$

The ratio β is sensitive to the nonspectator components in B-meson decay. Since semileptonic decay proceeds only by W emission, the semileptonic decay widths of the B^- and $\bar{B}^0$ should be equal [18]. Then β is equal to the ratio of the lifetimes of charged and neutral B mesons, τ_-/τ_0. The ratio ϕ determines the ratio of charged to neutral B mesons produced in $\Upsilon(4S)$ decay, and λ is required [19, 20] to obtain r from dilepton yields at the $\Upsilon(4S)$.

The ratio μ has been measured by ARGUS [21] using "semi-inclusive" semileptonic B decays, and CLEO [22, 23] using exclusive semileptonic B decays. After correcting these results for the 1990 Particle Data Group (PDG) branching fractions for D^* and D decays [24], the ARGUS value is $\mu = 0.98 \pm 0.22 \pm 0.13$ and the CLEO value is $\mu = 0.84 \pm 0.19 \pm 0.13$. These two results are in good agreement; we use their average

$$\mu = 0.90 \pm 0.17 \tag{5}$$

in this paper. These measurements are the only direct experimental information on the ratios, β, ϕ, λ, μ, or the ratio of the lifetimes of charged and neutral B mesons.

Inclusive single lepton and dilepton yields from B-meson decays at the $\Upsilon(4S)$ are proportional to

$$\langle b \rangle = f_0 b_0 + f_- b_- \tag{6}$$

and

$$\langle b^2 \rangle = f_0 b_0^2 + f_- b_-^2, \tag{7}$$

respectively. On the other hand, the average of the semileptonic branching ratios of charged and neutral B mesons,

$$b = \frac{b_0 + b_-}{2}, \tag{8}$$

is more interesting for comparisons to theoretical calculations, so we would like to interpret $\langle b \rangle$ as b. Of course, this interpretation is correct only if $f_- = f_0 = 0.5$, which is true only if $f_- + f_0 = 1$ [all $\Upsilon(4S)$ mesons decay to $B\bar{B}$] and $\phi = 1$. We now discuss the extent to which these relations may be correct.

The branching fraction $f_0 + f_-$ for $\Upsilon(4S) \to B\bar{B}$ is needed to determine the average branching fractions for B meson semileptonic decays from lepton yields from $\Upsilon(4S)$ data. In previous analyses of semileptonic B decays at the $\Upsilon(4S)$, it has implicitly been assumed that the $\Upsilon(4S)$ decays only to B^+B^- and $B^0\bar{B}^0$. If this assumption is relaxed, then

$$f_0 + f_- = 1 - f, \tag{9}$$

where f is the branching fraction for non-$B\bar{B}$ decays. By comparing dilepton to single lepton rates at the $\Upsilon(4S)$, an upper limit, $f < 0.13$, at a 95% confidence level (C.L.) was obtained [25]. This limit is very insensitive to assumptions about the origin of non-$B\bar{B}$ decays. In Sec. IV we show how dilepton and single lepton yields can be used to obtain the semileptonic branching fraction without any assumption about the value of f. Elsewhere in this paper we assume that f is negligible.

The near equality of the measured $\bar{B}^0$ and B^- masses [26–28] suggests that $\phi = 1$ is approximately correct, i.e., that $f_- \cong f_0$. Although the equality between f_- and f_0 would appear to be a consequence of isospin symmetry if the B^- and B^0 masses were equal, the theoretical situation is actually more complicated. First, naive Coulomb corrections [29] enhance the B^+B^- width leading to $\phi = 1.18$. However, a model calculation [30] that includes estimates of the momentum dependence of the $\Upsilon(4S)B\bar{B}$ vertex function and B^- and B^0 form factors indicates that the ratio is within about $\pm 5\%$ of 1.0. The effect of the $\Upsilon(4S)B\bar{B}$ vertex function on ϕ has been supported by another theoretical calculation [31]. In evaluating uncertainties in our experimental results, we will use

$$\phi = 1.00 \pm 0.05, \tag{10}$$

where the quoted error is an estimate of the theoretical uncertainty.

With the assumption that f is negligible and the theoretical result that $f_- \cong f_0$, the branching fraction $\langle b \rangle$ measured from a study of the inclusive lepton spectrum from $\Upsilon(4S)$ decay is essentially the average of the semileptonic branching fractions of charged and neutral B mesons.

The most straightforward way to measure the ratio b_-/b_0 requires separating charged and neutral B mesons. This can be done by reconstructing one "tag" B meson and seeing how often the other decays to a lepton. We achieve a reasonable tagging efficiency using the exclusive semileptonic B decay $\bar{B}^0 \to D^{*+}\ell^-\bar{\nu}$, since the branching fraction is relatively large. Unfortunately, most of the other low-multiplicity B decay modes are not useful due to their small branching fractions. One technique to overcome this limitation is to select decay modes which can be identified unambiguously without detecting all final-state particles. We successfully use partial reconstruction of the $\bar{B}^0 \to D^{*+}\pi^-$ events as a tag. Since we only tag neutral B mesons, we are only able to measure $\langle b \rangle/b_0$ directly.

The mixing parameter r is defined as the probability that a particle created as a B^0 will decay as a $\bar{B}^0$ divided by the probability that it will decay as a B^0. For $\Upsilon(4S)$ decays, where $B^0\bar{B}^0$ events are produced in a state of odd charge conjugation, the ratio between the number of events which decay as B^0B^0 or $\bar{B}^0\bar{B}^0$ (mixed events) and the number of events which decay as $B^0\bar{B}^0$ (unmixed events) is also equal to r, i.e.,

$$r = \frac{N(B^0B^0) + N(\bar{B}^0\bar{B}^0)}{N(B^0\bar{B}^0)}. \tag{11}$$

The value of r can be obtained from dilepton yields at the $\Upsilon(4S)$ using the ratio ρ,

$$\rho = \frac{N_{++} + N_{--}}{N_{+-}}, \tag{12}$$

of the number of like-sign dileptons $(N_{++} + N_{--})$ to the number of opposite-sign dileptons (N_{+-}). Then r is given by

$$r = \frac{(N_{++} + N_{--})(1+\lambda)}{N_{+-} - (N_{++} + N_{--})\lambda} = \frac{\rho(1+\lambda)}{1-\lambda\rho}. \tag{13}$$

The terms involving λ [Eq. (3)] are necessary to correct the opposite-sign dileptons for the contribution arising from charged B decay. The value $\lambda = 0.81 \pm 0.31$ is obtained from $\lambda = \mu^2/\phi$ and the values of μ and ϕ given in Eqs. (5) and (10), respectively. The ARGUS [19] and CLEO [20] measurements of ρ are $\rho = 0.091 \pm 0.026 \pm 0.014$ and $\rho = 0.076 \pm 0.020 \pm 0.012$, respectively; their average is

$$\rho = 0.082 \pm 0.019. \tag{14}$$

These values of λ and ρ imply

$$r = 0.176 \pm 0.053. \tag{15}$$

Originally both ARGUS and CLEO used $\lambda = 1.2$, suggested by an earlier assumption that $\phi \approx 1.2$; this value of λ gives a larger result for r.

$B^0\bar{B}^0$ mixing plays no role in our measurement of $\langle b \rangle$, but it is important in our measurements of b_0. If b_0 is measured using both mixed and unmixed events, the measurement is independent of r. However, the mixed event sample makes only a small contribution to the total, but makes a relatively large contribution to the statistical error. If only unmixed (right-sign) events are used in the measurement, the result is b_{0r}, the branching fraction for semileptonic decay to right-sign leptons. This result can be corrected for mixing using

$$b_0 = b_{0r}(1+r), \tag{16}$$

but this leads to systematic uncertainties due to the uncertainties in r. Furthermore, the measurements of r with the most statistical precision come from measurements of the ratio of the number of like-sign dileptons to the number of unlike-sign dileptons. However, using the value of r obtained directly from dilepton ratios to make this correction for b_0 would be circular, since the parameter λ given in Eq. (3) is required to obtain r from the dilepton ratio [19,20]. In addition, the measurement of b_{0r} itself requires estimation of backgrounds that depend on r. Since the backgrounds due to these events are small, the value of b_{0r} we obtain is very insensitive to the uncertainties in the measurement of ρ, or to variations of λ within reasonable limits. In any event, the sum of the backgrounds for right- and wrong-sign leptons is independent of r. In order to eliminate both the direct dependence of b_0 on r [Eq. (16)] and the indirect dependence due to the background estimates, we choose to present measurements of b_0 using both mixed and unmixed events. In Sec. V we show how measurements of b_{0r} can be combined with measurements of $\langle b \rangle$ and ρ and assumptions for f_- and f_0, to improve the statistical precision of the measurement of b_0 at the cost of modest additional systematic errors.

III. THE DATA SAMPLE

The results presented here have been obtained from 212 pb^{-1} of electron-positron annihilation data collected at the $\Upsilon(4S)$ resonance, denoted "on $\Upsilon(4S)$," and 101 pb^{-1} at energies just below $B\bar{B}$ threshold, referred to as "off $\Upsilon(4S)$." In the CLEO detector [32], charged particles are tracked inside a superconducting solenoid of radius 1.0 m, with a 1.0-T magnetic field parallel to the beam line. Three nested cylindrical drift chambers filled with a 50%–50% mixture of argon-ethane gas are used to measure momenta and specific ionization (dE/dx) for charged particles. The innermost part of the tracking system is a three-layer straw-tube vertex chamber [33] with an rms position accuracy of 70 μm. The middle 10-layer drift chamber [34] and the large 51-layer drift chamber [35] measure both position and specific ionization (dE/dx). The drift distance resolutions are 90 μm and 110 μm, respectively. Position information along

the beam direction is provided by 11 small-angle stereo layers in the large drift chamber, and cathode strips in both. The momentum resolution achieved by this system is $(\sigma_p/p)^2 = (0.23\%p)^2 + (0.7\%)^2$, with p in GeV/c. It is determined from Bhabha scattering and $e^+e^- \to \mu^+\mu^-$ events, and by the observed mass resolution for $K^0_S \to \pi^+\pi^-$, $\Lambda \to p\pi^-$, $\phi \to K^+K^-$, $D^0 \to K^-\pi^+$, $\psi \to \mu^+\mu^-$, and $B^- \to D^0\pi^-$ decays. The dE/dx determinations made in the 10- and 51-layer drift chambers provide particle-identification information. The respective precisions of these measurements are 14% and 6.5%.

Outside the solenoidal magnet several detector components are arrayed for particle identification. These include pressurized proportional chambers for additional specific ionization measurements, plastic scintillators for time-of-flight particle identification, and lead-proportional tube electromagnetic calorimetry. Surrounding these components is a steel hadron filter of thickness 0.6 to 1.0 m (4 to 7 interaction lengths). Muons are detected by a system of crossed drift-chamber planes mounted on the outside of this absorber. More details about the performance of these systems are provided in the discussion of lepton identification below.

Our standard hadronic event selection criteria have been described in detail elsewhere [36]. Briefly, for this analysis there are six primary requirements:

(i) Accepted hadronic events are required to have at least four well-reconstructed charged tracks.

(ii) The reconstructed event vertex is required to lie within 5 cm of the nominal interaction point along the beam axis and within 2 cm in the plane perpendicular to the beam direction.

(iii) A minimum value for visible charged energy (charged tracks plus energy deposits in the calorimeter not matched to charged tracks) of 30% of the center-of-mass energy is demanded.

(iv) The total energy deposited in the electromagnetic calorimeter is required to be between 0.5 and 7.0 GeV.

(v) Since the momentum imbalance in most hadronic events is small, the ratio R_1 of Fox-Wolfram moments [37] is required to be less than 0.45.

(vi) Events with charged particle multiplicity of no more than 6 may not have two oppositely directed high-momentum showering tracks. This cut suppresses radiative Bhabha events where the photon converted in the beam pipe.

The overall efficiency of these hadronic event-selection cuts for generic $B\bar{B}$ events is 96%.

Our lepton identification criteria [20, 36, 38] have been described elsewhere. Here we summarize the criteria used in selecting the inclusive lepton data samples; less stringent electron identification requirements, described in the appropriate sections below, are used in selecting the electrons for the dilepton data sample and the tagged measurements of B^0. The dE/dx measurements in the main drift chamber (solid angle $0.80 \times 4\pi$) provide about 3 standard-deviation separation between electrons and pions in the momentum interval between 1.4 and 2.4 GeV/c. Within a more restricted solid angle ($0.48 \times 4\pi$), the electromagnetic calorimeters, pressurized proportional chambers, and time-of-flight scintillators provide additional discrimination. We use two non-overlapping electron data samples: Sample A includes electrons with momentum above 0.5 GeV/c within the solid angle of the calorimeters. Sample B consists of electrons with momenta above 1.7 GeV/c outside of the solid angle for sample A, but within the solid angle of the drift chamber. The two data samples are combined in the fits to the lepton spectra. For each electron candidate we examine several quantities, including the ratio of the total energy deposited in the calorimeter to the measured momentum, the fraction of the energy deposited in the front part of the calorimeter, the width of the shower, and the measured dE/dx pulse heights. By comparing the observed values with distributions obtained from a large sample of electrons from kinematically selected radiative Bhabha events, we calculate an electron likelihood L_e. Similarly, using distributions obtained from $\Upsilon(1S)$ decays which contain very few electrons, we determine a hadron likelihood L_h. For the inclusive electron spectrum, we accept candidates with $\ln(L_e/L_h) \geq 4$. The electron efficiencies are determined using electrons from radiative Bhabha events. The hits of these tracks are superimposed on hadronic events to provide a realistic approximation of B-meson semileptonic decay events. The particle-identification efficiencies for electrons in the inclusive lepton data sample are illustrated in Fig. 3. Hadrons misidentified as leptons are called "fake" leptons. For electron sample A, the probability of misidentifying a hadron as an electron (fake probability) was determined using $\Upsilon(1S)$ events. For sample B, the fake probability was determined using particles from $\Upsilon(4S)$ events identified as hadrons using the devices other than the drift chamber within the solid angle of sample A. The momentum dependences of the fake probabilities for both electron samples are illustrated in Fig. 4.

Muons are identified by seeking matches between high-

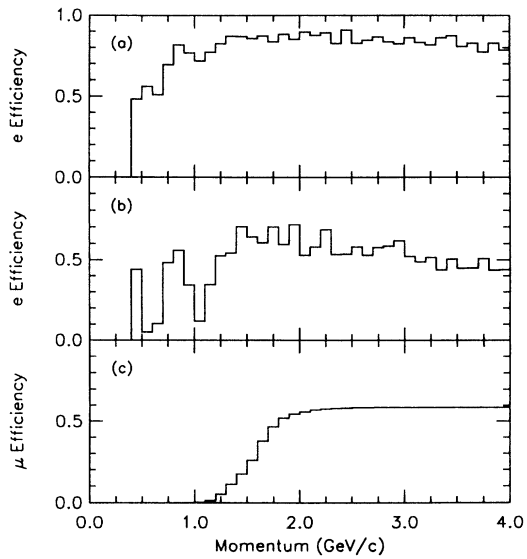

FIG. 3. The lepton identification efficiencies as functions of the lepton momentum in the inclusive lepton data sample; (a) and (b) are the efficiencies for electrons in sample A and sample B, respectively, and (c) is the efficiency for muons within the solid angle of the muon drift chambers.

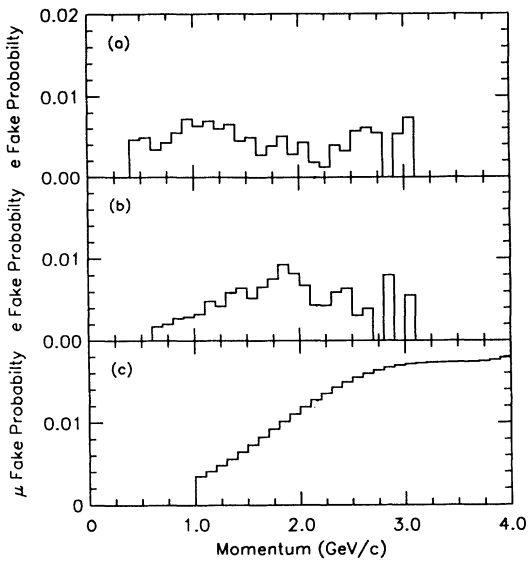

FIG. 4. The fake probabilities (probabilities that hadrons are misidentified as leptons) as functions of the momentum of the hadron; (a) and (b) are the fake probabilities for hadrons within the solid angles of electron samples A and B, respectively, and (c) is the fake probability for hadrons within the solid angle for muon detection.

momentum charged tracks and hits in the muon drift chambers. The solid angle subtended by the muon chambers is $0.76 \times 4\pi$. The minimum muon momentum for penetration through the absorber varies with direction between 1.2 and 2 GeV/c. The efficiency for identifying a muon is determined from $e^+e^- \rightarrow \mu^+\mu^-$ events and Monte Carlo calculations, and the probability that a hadron is misidentified as a muon is determined using $\Upsilon(1S)$ events. The efficiency and fake probability as functions of the momentum are illustrated in Figs. 3 and 4, respectively.

The numbers of events which passed our criteria are shown in Table I. The $\Upsilon(4S)$ yields are obtained by scaling the off-$\Upsilon(4S)$ (continuum) data by the factor

$$f_{\mathcal{L}} = 2.08 \pm 0.01, \tag{17}$$

and subtracting them from the on-$\Upsilon(4S)$ data. This factor is the ratio of the luminosities of the two data samples, corrected for the $1/s$ dependence of the continuum annihilation cross section. The lepton momentum spectra for $\Upsilon(4S)$ decays are similarly obtained by a bin-by-bin subtraction of the off-$\Upsilon(4S)$ lepton momentum distribution from the on-$\Upsilon(4S)$ momentum distribution.

IV. MEASURING THE SEMILEPTONIC BRANCHING FRACTION

A. The inclusive lepton spectra

The procedure followed [39] is basically the same as has been used in past CLEO measurements [12, 13]. We assume that the contribution of non-$B\bar{B}$ decays to the lepton spectrum from $\Upsilon(4S)$ decays is negligible. This implies that there will be two dominant components in the observed lepton spectrum.

(i) Primary leptons. The first component is lepton production from direct semileptonic decays of B mesons. Both $b \rightarrow c\ell\nu$ and $b \rightarrow u\ell\nu$ will contribute, but the errors of this measurement make it largely insensitive to the small magnitude of the latter [40]. For consistency, we have included $b \rightarrow u\ell\nu$ in our fits to the lepton spectra. The $b \rightarrow c\ell\nu$ decays, $\bar{B} \rightarrow (D, D^*, D^{**})\ell^-\bar{\nu}$, dominate the observed lepton yield above 1.4 GeV/c. As described below, models that differ greatly in the way they treat quark hadronization are all successful in predicting the $b \rightarrow c\ell\nu$ lepton spectrum.

(ii) Secondary leptons. The second component is leptons from the sequential process $b \rightarrow c \rightarrow s\ell\nu$ in which a B decays into a D, and the daughter D decays semileptonically. These decays produce a softer lepton spectrum than that produced by primary leptons.

The momentum spectra of these two sources are sufficiently different to allow determination of both the semileptonic branching fraction $B(\bar{B} \rightarrow X\ell^-\bar{\nu})$ and the product branching fraction

$$B(b \rightarrow c \rightarrow s\ell\nu) \equiv B(\bar{B} \rightarrow DX)B(D \rightarrow Y\ell\nu), \tag{18}$$

from a fit of the inclusive lepton momentum spectrum.

Before the lepton momentum spectra from $\Upsilon(4S)$ decays can be fitted, the contribution of fake leptons must be subtracted. We calculate the fake lepton spectrum by weighting the observed momentum distribution for hadron tracks by measurements of the lepton misidentification probabilities shown in Fig. 4. For the electron sample A and the muon sample, we obtain the fake spectrum from $\Upsilon(1S)$ data, where only a very few leptons are expected. Since the relative fractions of pions, kaons, and protons produced by $\Upsilon(1S)$ and $\Upsilon(4S)$ decays are not the same, the misidentification probabilities are different for these two data samples. In order to estimate this effect we have also directly measured the misiden-

TABLE I. The luminosities, lepton yields, and number of hadronic events for the on $\Upsilon(4S)$, off $\Upsilon(4S)$, and net $\Upsilon(4S)$ data samples.

	On $\Upsilon(4S)$	Off $\Upsilon(4S)$	$\Upsilon(4S)$ Yield
Luminosity (pb^{-1})	212	101	
Electron events	48 440	8 461	30 841± 292
Muon events	15 359	2 692	9 760± 164
Hadronic events	818 071	281 398	233 044±1 426

tification probabilities using pions, protons, and kaons identified in the decays $K_S^0 \to \pi^+\pi^-$, $\Lambda \to p\pi^-$, and $D^0 \to K^-\pi^+$ tagged with $D^{*+} \to D^0\pi^+$. The fake rate determined from these decays is about 20% higher than that obtained from $\Upsilon(1S)$ data; this difference dominates the systematic error in the fake rate.

After the fake subtraction, the resulting lepton spectra are corrected for track-reconstruction and lepton-identification efficiencies. The track reconstruction efficiency is determined to be $(99 \pm 1)\%$ from Monte Carlo calculations. The resulting lepton spectra are normalized to the observed number of $B\bar{B}$ pairs. The spectra must be further corrected by the ratio of the efficiency for detecting semileptonic events (ϵ_{SL}) and ordinary $B\bar{B}$ events ($\epsilon_{B\bar{B}}$). This ratio is less than one because the lower-multiplicity semileptonic events more often fail the requirement that the number of reconstructed tracks be greater than five. From Monte Carlo calculations, we estimate $\epsilon_{SL}/\epsilon_{B\bar{B}} = 0.98 \pm 0.01$. Finally, we subtract the lepton spectra from $B \to \psi X$, $\psi \to \ell^+\ell^-$, which contributes [41] $(0.16 \pm 0.04)\%$, and $B \to \tau X$, $\tau \to \nu_\tau \ell \nu_\ell$, which contributes [42] $(0.6 \pm 0.4)\%$. The electron and muon momentum spectra resulting after all corrections are shown in Fig. 5.

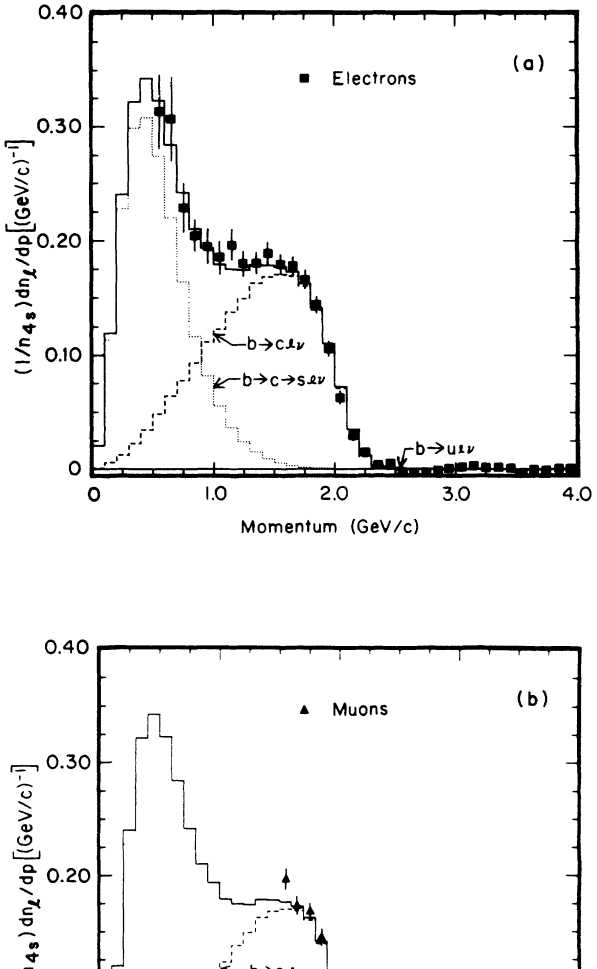

FIG. 5. The momentum spectra from B meson decay for electrons (a) and muons (b). The histogram represents the fitted contributions of the ACCMM model described in the text. The dashed, dotted, and solid histograms are the contributions from $b \to c\ell\nu$, $b \to c \to s\ell\nu$, and their sum, respectively. The $b \to u\ell\nu$ contribution is too small to be visible in the figures; the arrows indicate the end-point region where it dominates.

B. The semileptonic branching fraction from fits to the lepton spectra

The momentum spectra for both primary and secondary leptons are required to fit our data; we use two models of semileptonic B and D decay to calculate these spectra. These two models are distinguished from other available models in their calculation of the entire spectrum for semileptonic B decay.

(i) The Altarelli-Cabibbo-Corbò-Maiani-Martinelli (ACCMM) refined free-quark model. The ACCMM [43] model is a refined free-quark model that includes corrections for gluon emission [44]. There are several unknown parameters required to describe a decay in this model: the mass of the spectator quark in the parent meson, the mass of the c, u, or s quark in the daughter meson resulting from the weak decay, and a Fermi momentum p_F which describes the momentum distribution of the spectator quark in the parent meson. We use the ACCMM model with three sets of the mass and Fermi-momentum parameters to describe the data, one each for $b \to c\ell\nu$, $b \to u\ell\nu$, and $c \to s\ell\nu$ decays. The lepton spectrum is not sensitive to the value of the spectator quark mass, which we fix to be 150 MeV/c^2 for all three decays. The lepton spectrum is sensitive to p_F and m_c, which we include as free parameters for $b \to c\ell\nu$ decays; they are highly correlated [14] and their uncertainties dominate the statistical error in the fits to the ACCMM model. For $b \to u\ell\nu$ decay, we fix the mass of the u quark to be the same as the mass of the spectator quark and the Fermi momentum to be the same as the Fermi momentum in $b \to c\ell\nu$ decays. The results are very insensitive to the values of the $b \to u\ell\nu$ parameters. In $c \to s\ell\nu$ decays, the mass of the s quark, m_s, and its Fermi momentum, q_F, are not well constrained by our data. From a separate fit of the ACCMM model to the measured lepton spectrum from semileptonic D decays [45], we obtain $m_s = 50^{+196}_{-50}$ MeV/c^2 and $p_F = 282 \pm 94$ MeV/c.

(ii) The Isgur-Scora-Grinstein-Wise (ISGW) form-factor model. The ISGW [46] model is based on calculations of the form factors in a nonrelativistic quark model for the particular exclusive final states, $\bar{B} \to (D, D^*, D^{**})\ell^-\bar{\nu}$. In principle there are no free parameters in this model. The relative branching fractions cal-

culated by ISGW for the D, D^*, and D^{**} final states are 27%, 62%, and 11%, respectively. Previously, we have measured [22] the exclusive semileptonic branching fractions for the D and D^* final states. The ratio of the two agrees well with the prediction of the ISGW model, but the error is too large to provide a significant test of the model. However, the sum of the exclusive D and D^* branching fractions is only $(65 \pm 12)\%$ of the average B semileptonic branching fraction. This result suggests that the semileptonic branching fraction for the D^{**} final state might be as large as 35%. As described below, we have studied the sensitivity of our inclusive results to variations of the relative fraction of D^{**}.

Electroweak radiative corrections to these models are significant; we calculate them in the B-meson rest-frame using a model-independent prescription [29] which includes the effects of short-distance loop corrections and soft virtual and real photons. The correction varies significantly over the momentum range of our measurement; its magnitude at the high-momentum end point approaches 10% for electrons and 3% for muons. The branching fractions obtained using these radiative corrections are larger by a factor of about 1.01 than those obtained without applying the radiative corrections.

To produce primary lepton spectra, we apply radiative corrections to the $b \to c\ell\nu$ and $b \to u\ell\nu$ spectra from the models, boost them to the $\Upsilon(4S)$ rest frame, and fold in a detector response function generated from our detector Monte Carlo simulation. To produce secondary lepton spectra, the $c \to s\ell\nu$ spectra from the models are radiatively corrected, and then folded with our previously reported momentum spectrum for D mesons produced in B decays [41, 47].

The sums of the contributions of primary and secondary leptons are fit to the data. Fits are made separately to the electron spectrum from 0.5–2.8 GeV/c, and to the muon spectrum from 1.5–2.8 GeV/c. For the muons, the parameters of the secondary spectrum are held fixed at the values determined by the electron fit, since the fraction of secondary leptons above 1.5 GeV/c is too small to provide a constraint on itself. In addition, we simultaneously fit the electron and muon spectra; these simultaneous fits are denoted by ℓ.

The results of these fits are illustrated in Figs. 6(a) and 6(b), and are given in Table II. The branching fractions, $B(b \to q\ell\nu)$ listed are the sum of the $b \to c\ell\nu$ and $b \to u\ell\nu$ contributions. The two models are in agreement but the ACCMM model seems to fit the data substantially better than the ISGW model does. For the ACCMM model, the best fit values for m_c and p_F of the $b \to c\ell\nu$ component are given in Table III. The statistical errors for the branching fractions in the ACCMM model are slightly larger than those for the ISGW model because these ACCMM model parameters are determined in the fits. The systematic errors are due to the uncertainties in the lepton identification efficiencies, the track-reconstruction efficiency, the ratio of the $\Upsilon(4S)$ luminosity to continuum luminosity, the ratio of semileptonic to hadronic efficiencies, radiative corrections, the fake probability, and the contributions of $B \to \psi X$ and $B \to \tau X$. The fractional errors in these parameters and their contributions to the systematic errors in the $B(b \to c\ell\nu)$ branching fractions are listed in Table IV.

The average [48] of the electron and muon results from the two models is $B(\bar{B} \to X\ell^-\bar{\nu}) = (10.2 \pm 0.2 \pm 0.4 \pm 0.3)\%$, where the first error is statistical and the second error is the experimental systematic error from Table IV. The third error is the variation of these two models from their average.

These results for the B semileptonic branching fraction are compared to recent Crystal Ball [11], ARGUS [14], CUSB [15], and previous CLEO [13, 49] results in Table V. There is excellent agreement among the ARGUS, CUSB, and both CLEO results, but these results are not in good agreement with the Crystal Ball result.

The branching fractions for $b \to c \to s\ell\nu$ decays given in Table II are in good agreement with $(9.8 \pm 1.5)\%$ estimated using the PDG values [24] of the semileptonic branching fractions for D mesons and a recent CLEO measurement [27, 28] of the $B \to DX$ branching fractions.

In our earlier measurement [22] of the exclusive semileptonic decays, $\bar{B} \to D\ell^-\bar{\nu}$ and $\bar{B} \to D^*\ell^-\bar{\nu}$, we

TABLE II. Results of fits of the ACCMM and ISGW models to the inclusive lepton spectrum. The first error is statistical and the second is the experimental systematic error. The branching fractions, $B(b \to q\ell\nu)$ are the sum of the $b \to c\ell\nu$ and $b \to u\ell\nu$ contributions. The data labeled "ℓ" refer to simultaneous fits to the e and μ data, yielding the *average* of the electron and muon branching fractions.

Model	Data	$\chi^2/N_{\rm DF}$	$B(b \to q\ell\nu)$ (%)	$B(b \to c \to s\ell\nu)$ (%)
ACCMM	e	11.4/18	10.5±0.2±0.3	9.7±0.8±0.6
	μ	3.9/ 9	10.7±0.7±0.7	
	ℓ	17.1/31	10.5±0.2±0.4	9.7±0.8±0.6
ISGW	e	26.2/20	10.1±0.2±0.3	11.1±0.7±0.7
	μ	16.0/11	9.7±0.3±0.6	
	ℓ	44.0/33	9.9±0.1±0.4	11.3±0.7±0.6

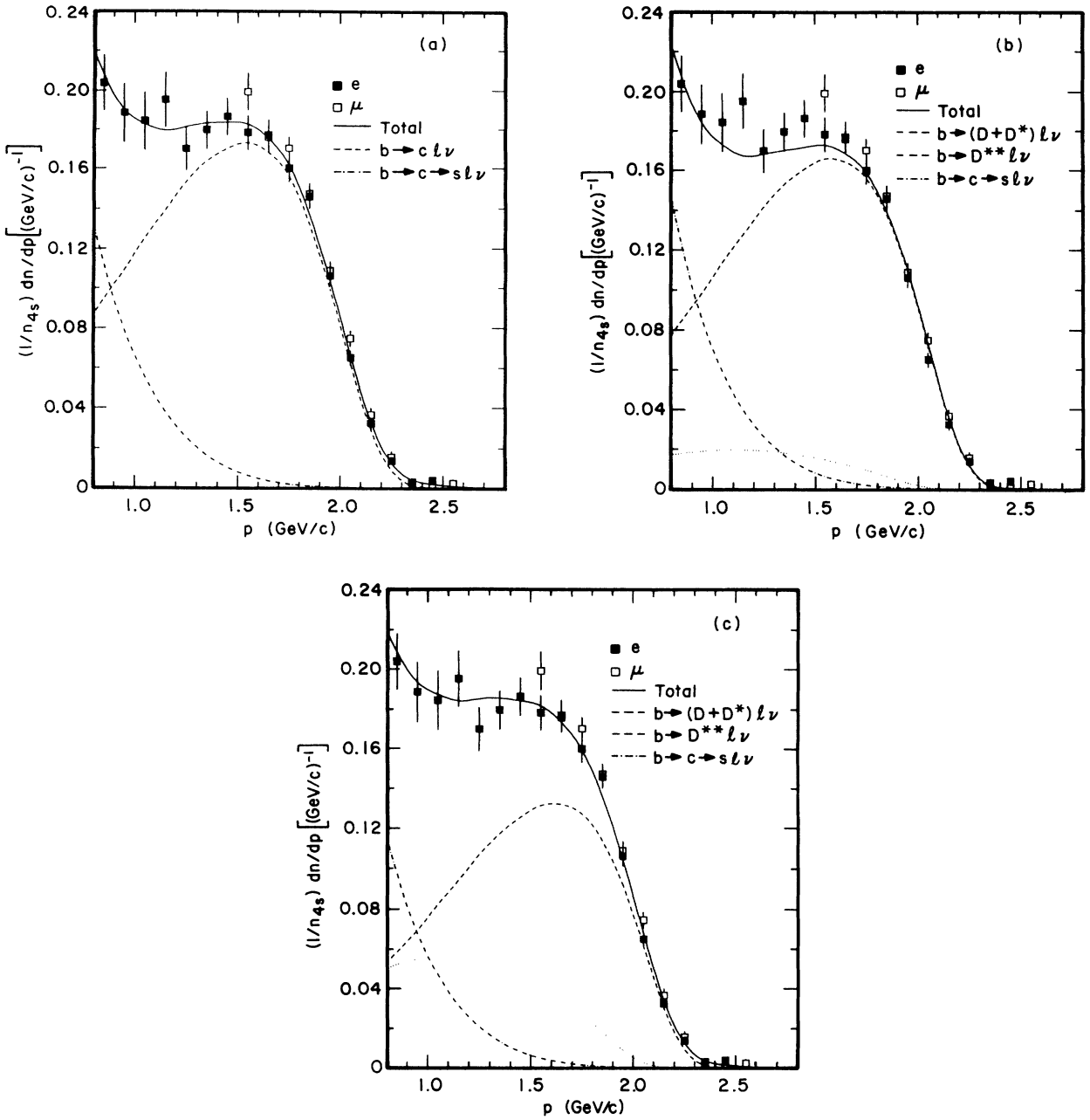

FIG. 6. The electron and muon momenta spectra for $p_\ell \geq 0.8$ GeV/c and the fits to these data; (a) is the ACCMM fit, (b) is the ISGW fit, and (c) is the ISGW** fit where the D^{**} fraction is allowed to vary. The total fit and the $b \to c\ell\nu$ and $b \to c \to s\ell\nu$ components are illustrated as indicated. For clarity, the $b \to u\ell\nu$ components are not included.

found that the sum of the branching fractions for the two exclusive modes was only (65±12)% of the total semileptonic branching fraction. This suggests that the reason for the relatively poor fit to the ISGW model may be that the branching fraction to higher mass charm states may be much larger than the 11% branching fraction for $\bar{B} \to D^{**}\ell^-\bar{\nu}$ predicted by the model. This motivated us to fit the data to the ISGW model allowing the D^{**} fraction to vary relative to the sum [50] of the D and D^* contributions (we refer to this fit with a variable D^{**} fraction as the ISGW** model). The best-fit results are

TABLE III. Best-fit values of m_c and p_F for the $b \to c\ell\nu$ component of the ACCMM model. The data labeled "ℓ" refer to the simultaneous fit to the e and μ data. The first error is statistical and the second is systematic.

Data	m_c (MeV/c^2)	p_F (MeV/c)
e	1717± 80±16	247± 82±16
μ	1600±105±18	385±135±27
ℓ	1673± 58±24	298± 59±27

TABLE IV. Contributions to the experimental systematic errors for the $b \to q\ell\nu$ branching fractions listed in Table II. For each parameter used in determining the semileptonic branching fractions, the fractional error in the parameter is listed along with its contribution to the systematic error in the branching fraction, B.

Parameter	Fractional error in parameter (%)		Contribution to systematic error in B (%)	
	e data	μ data	e data	μ data
Lepton identification efficiency	2	5	0.2	0.6
Track-reconstruction efficiency	1	1	0.1	0.2
Luminosity ratio - $f_{\mathcal{L}}$	0.5	0.5	0.1	0.1
$\epsilon_{SL}/\epsilon_{B\bar{B}}$	1	1	0.1	0.1
Radiative corrections			0.1	0.05
Fake probability	20	20	0.04	0.04
$B \to \psi X$	25	25	0.03	0.05
$B \to \tau X$	67	67	0.02	0.05
Sum in quadrature			0.3	0.6

illustrated in Fig. 6(c) and given in Table VI; the D^{**} fraction resulting from the fit is $(32 \pm 5)\%$, comparable to our result from exclusive decays. In addition, inclusion of this single parameter to the fit leads to a decrease of 25 in the χ^2. However, the semileptonic branching fraction for B decays obtained from the ISGW model fit increases from 9.9% to 11.2%. Comparison of Tables II and VI shows that this larger B-meson semileptonic branching fraction is at the expense of the contribution from $b \to c \to s\ell\nu$ decays, which decreases by a comparable amount. The substantial decrease in χ^2 when the D^{**} fraction is allowed to float indicates that the ISGW model does not adequately describe the contributions due to charm states above the D and D^*. Although there is no firm evidence that the shape of the ISGW D^{**} spectrum adequately models the low-momentum (high charm mass) states, we nevertheless are compelled to quote the ISGW** fit instead of the ISGW fit as the result of fitting the ISGW model to our data. The average of the ACCMM and ISGW** branching fractions is

$$B(\bar{B} \to X\ell^-\bar{\nu}) = (10.8 \pm 0.2 \pm 0.4 \pm 0.4)\%, \qquad (19)$$

where the first error is statistical, the second is the experimental systematic error, and the third is an estimate of the systematic error due to uncertainties in the models.

Figure 7 shows the results of the ACCMM, ISGW, and ISGW** fits near the $b \to c\ell\nu$ end point. The $b \to u\ell\nu$ contributions of the ACCMM and ISGW** fits are consistent with the data above the $b \to c\ell\nu$ end point, while the $b \to u\ell\nu$ contribution for the ISGW fit is much smaller than the data indicate. The suppression of this component in the ISGW fits is due to the fact that the small D^{**} fraction in the model forces the hard D and D^* contributions to be larger near the $b \to c\ell\nu$ end point, which in turn reduces the $b \to u\ell\nu$ contribution allowed in the fit. This indicates that the ISGW model is inconsistent with the data in the region of $b \to u\ell\nu$ dominance as well as in the region between $b \to c\ell\nu$ and $b \to c \to s\ell\nu$

TABLE V. Summary of recent measurements of the semileptonic branching fraction. When both electron and muon results were available, the average is quoted.

Experiment	$B(b \to q\ell\nu)$ (%)	
	ACCMM Model	ISGW Model
Present results	10.5±0.2±0.4	9.9±0.1±0.4
ARGUS [14]	10.2±0.4±0.2	9.9±0.4
CUSB [15]	10.0±0.4±0.3	10.0±0.4±0.3
CLEO [13, 49]	10.1±0.3±0.4	10.1±0.3±0.4
Crystal Ball [11]	12.0±0.5±0.7	11.9±0.4±0.7

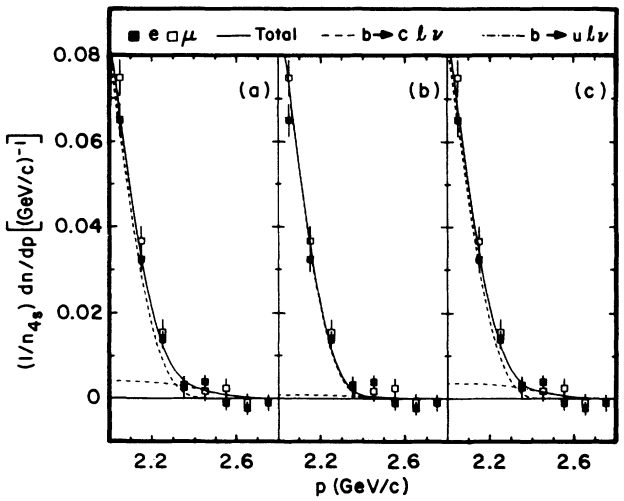

FIG. 7. The electron and muon momentum spectra in the interval, $2.0 \leq p_\ell \leq 2.8$ GeV/c; (a) is the fit to the ACM model, (b) is the fit to the ISGW model, and (c) is the fit to the ISGW** model where the D^{**} fraction is allowed to vary. The $b \to c\ell\nu$ and $b \to u\ell\nu$ components are shown along with the total. The $b \to c \to s\ell\nu$ contribution is negligible in this momentum interval and has not been included in the figures.

TABLE VI. Results of fits to the inclusive lepton spectrum using the ISGW model with the fraction of final-state D^{**} allowed to vary. The ratio of the amount of D^* to D is fixed at 2.3. The data labeled "ℓ" refer to simultaneous fits to the e and μ data, resulting in the *average* of the electron and muon branching fractions. The first error is statistical and the second is the experimental systematic error.

Data	χ^2/N_{DF}	$D/D^*/D^{**}$ ratios (%)	$B(b \to q\ell\nu)$ (%)	$B(b \to c \to s\ell\nu)$ (%)
e	13.8/19	22/49/29	11.1±0.3±0.3	9.3±0.9±0.6
μ	3.7/10	19/43/38	11.7±0.6±0.7	
ℓ	19.1/32	21/47/32	11.2±0.3±0.4	9.0±0.8±0.6

dominance. The $b \to u\ell\nu$ contributions of the ACCMM and ISGW** models are consistent, but neither is very consistent with that of the ISGW model.

We conclude that the ISGW model with a D^{**} contribution of 11% does not adequately describe the inclusive electron spectrum from B meson decay. We have included the results obtained with this model in Table II and elsewhere in this paper to facilitate comparison with other measurements.

C. Semileptonic B decay to baryons

The measurements of the B-meson semileptonic branching fraction are somewhat lower than theoretical expectations based on the spectator model [10,16], which generally predict semileptonic branching fractions above 12%. However, some care must be taken in interpreting this statement, because of the possibility that our procedure fails to account for some subset of semileptonic decays, such as $\bar{B}^0 \to \Lambda_c^+ \bar{n}\ell^-\bar{\nu}$. These leptons would be expected to have a soft momentum spectrum, though the exact shape of this spectrum has neither been measured nor predicted. In principle, decays of this type would be included in the lepton spectrum predicted by the ACCMM model, since it sums over all possible final hadron states. Decays of this type are explicitly not included in the ISGW model, so we must estimate how large their contribution could be. We estimate an upper limit for this effect by combining the CLEO measurement [51] of the inclusive branching fraction $B(\bar{B} \to \Lambda_c^+ X) = (6.4 \pm 1.1)\%$, with the expected semileptonic branching fraction for these decays. The latter is expected to be approximately 20%, since the virtual W is not sufficiently energetic to decay into $\bar{c}s$ or $\tau\nu$. From these considerations we conclude that this channel could contribute no more than an additional 1.3% to the semileptonic branching fraction. Furthermore, it is possible that Λ_c production in B decays might not be dominantly from spectator diagrams, in which case the true branching fraction could be significantly less than 1.3%. ARGUS has measured [14] an upper limit $B(B \to X\bar{p}e^+\nu_e) < 0.16\%$ (90% C.L.) for B decays to an antiproton and positron; this shows that the fraction of the inclusive lepton spectrum coming from semileptonic decays involving baryons is indeed small. Therefore, we neglect the baryon contribution to semileptonic B decays.

D. Calculating $|V_{cb}|$ and $|V_{ub}/V_{cb}|$ from the semileptonic branching fraction

We obtain the CKM matrix element $|V_{cb}|$ from the semileptonic branching ratio using

$$\Gamma_{SL} = \gamma_c|V_{cb}|^2 + \gamma_u|V_{ub}|^2. \tag{20}$$

where the reduced widths, γ_c and γ_u, are obtained from the ACCMM and ISGW models. We calculate γ_c for the ISGW model [52] and the ACCMM model [53] from the same model parameters used in obtaining the semileptonic branching fractions. The resulting values of γ_c are given in Table VII. To obtain the semileptonic width, we use our measured semileptonic branching fractions

TABLE VII. Values of $|V_{cb}|$ obtained from the ISGW and ACCMM models using the measured semileptonic branching fractions $B(b \to c\ell\nu)$, the average B lifetime, and the values of γ_c from the models. The first error for $|V_{cb}|$ is derived from the errors for the branching fraction and τ_B; the second error is due to the quoted uncertainty in γ_c. For the ISGW model, two values of $|V_{cb}|$, corresponding to 11% and 32% D^{**} contributions are included.

Model	γ_c (ps^{-1})	$B(b \to c\ell\nu)$ (%)	$\lvert V_{cb}\rvert$
ACCMM	37± 7	10.3±0.2±0.4	0.048±0.002±0.005
ISGW – 11% D^{**}	41± 8	9.8±0.2±0.4	0.044±0.002±0.004
ISGW** – 32% D^{**}	50±10	11.0±0.3±0.4	0.042±0.002±0.004

for $b \to c\ell\nu$. For the B-meson lifetime, we use [54] $\tau_B = 1.23 \pm 0.08$ ps, the average of the PDG value [24], $\tau_B = 1.18 \pm 0.11$ ps, and a more recent measurement, $\tau_B = 1.29 \pm 0.06 \pm 0.10$ ps, from the ALEPH Collaboration [55]. These branching fractions, and the resulting values for $|V_{cb}|$, are given in Table VII. They are in good agreement with previous CLEO measurements [22, 56] obtained from exclusive $\bar{B} \to D(D^*)\ell\bar{\nu}$ decays and with measurement of inclusive semileptonic decays from ARGUS [14]. The values of $|V_{cb}|$ for the two versions of the ISGW model are nearly identical.

Extraction of $|V_{ub}|$ is hampered by large experimental and theoretical uncertainties in the small $b \to u\ell\nu$ contribution. However, many of these are avoided by calculating $|V_{ub}/V_{cb}|$ instead. We do this using the ratios of γ_u/γ_c and $B(b \to u\ell\nu)/B(b \to c\ell\nu)$. These parameters, and the resulting values of $|V_{ub}/V_{cb}|$, are given in Table VIII for the ACCMM model, and the ISGW model with 11% and 32% D^{**} fraction. They are in agreement with the previous CLEO measurement [40] of $|V_{ub}/V_{cb}|$, using the same data sample. These new measurements are presented to show that determining $|V_{ub}/V_{cb}|$ from fits to the lepton spectra using the ACCMM and ISGW** models is consistent with the previous measurements. The values given here *do not* supersede the previous CLEO measurement of $|V_{ub}/V_{cb}|$ because the new measurements are much more sensitive to the $b \to c\ell\nu$ spectrum than the earlier results obtained using only data above or just below the $b \to c\ell\nu$ end point.

E. The semileptonic branching fraction from dilepton yields

The ratio of dilepton to single lepton yields at the $\Upsilon(4S)$ can be used to measure b [Eq. (8)], the average of the semileptonic branching fractions of charmed and neutral B mesons. We assume that the lepton contribution from possible non-$B\bar{B}$ decays of the $\Upsilon(4S)$ are negligible; this assumption is examined carefully elsewhere [25]. The single and dilepton yields from the $\Upsilon(4S)$ are, respectively,

$$N_\ell = 2\epsilon_\ell N_{4S}(f_0 b_0 + f_- b_-), \tag{21}$$

$$N_{\ell\ell} = g\epsilon_\ell^2 N_{4S}(f_0 b_0^2 + f_- b_-^2). \tag{22}$$

In these expressions, N_{4S} is the number of $\Upsilon(4S)$ events, ϵ_ℓ is the efficiency for detecting a single lepton, and $g = 0.98 \pm 0.02$ is a factor, estimated from a Monte Carlo calculation, accounting for the differences between ϵ_ℓ^2 and the efficiency for detecting dileptons. The ratio

$$R_{\ell\ell} = \frac{2N_{\ell\ell}}{g\epsilon_\ell N_\ell} = \frac{f_0 b_0^2 + f_- b_-^2}{f_0 b_0 + f_- b_-} = \frac{\langle b^2 \rangle}{\langle b \rangle}, \tag{23}$$

determined from measured single lepton and dilepton yields and the known lepton efficiencies, is sensitive to b, but is very insensitive [57] to f or to the ratios ϕ and β, if the latter two quantities are near 1. In terms of $R_{\ell\ell}$, ϕ [Eq. (2)], and μ [Eq. (4)], b is given by

$$b \equiv \frac{b_0 + b_-}{2} = c(\phi, \mu) R_{\ell\ell}, \tag{24}$$

where $c(\phi, \mu)$ is

$$c(\phi, \mu) = \frac{(1+\mu)(\phi+\mu)}{2(\phi+\mu^2)}. \tag{25}$$

In fact, the derivatives of $c(\phi, \mu)$ with respect to ϕ and μ are zero at $\phi = \mu = 1$. We use the theoretical estimate, $\phi = 1.00 \pm 0.05$ [see the discussion of Eq. (10)], and the average of the ARGUS and CLEO values of μ from Eq. (5). These give

$$c(\phi, \mu) = 0.997\ ^{+0.003}_{-0.021}, \tag{26}$$

where the asymmetry in the errors is due to the fact that the measured value of μ is not equal to 1. Note that these errors are comparable to the fractional errors in the measurements of $\langle b \rangle$ given in Tables II and VI.

Event and lepton selection followed the same procedures outlined above. For this analysis, leptons in the momentum interval, $1.4 \le p_\ell \le 2.5$ GeV/c are used [58], but it is necessary to handle some backgrounds differently. The single and dilepton yields are corrected for backgrounds as follows.

(i) Continuum leptons. The yields, $N_{4S\ell}$, of direct leptons from $\Upsilon(4S)$ events are obtained by subtracting the lepton yields from off $\Upsilon(4S)$ events from those of on $\Upsilon(4S)$ events using the luminosity ratio, $f_{\mathcal{L}}$ in Eq. (17).

(ii) Fake leptons. The contributions, $n_{f\ell}$, of fake leptons to the single lepton yields are estimated using the momentum-dependent fake probabilities illustrated in Fig. 4, and subtracted from the single lepton yields. The contribution of fake leptons to the dilepton yields are dominated by real-fake combinations, so the estimated

TABLE VIII. Values of $|V_{ub}/V_{cb}|$ obtained from the ISGW and ACCMM models using the ratio $R_{uc} = B(b \to u\ell\nu)/B(b \to c\ell\nu)$, and the ratio of γ_u and γ_c from the models. The first error for $|V_{ub}/V_{cb}|$ is derived from the errors for the branching fractions; the second error is due to the quoted uncertainty in widths. For the ISGW model, two values of $|V_{cb}|$, corresponding to 11% and 32% D^{**} contributions, are included. As noted in the text, the results given here *do not* supersede the previous CLEO results given in Ref. [40].

Model	γ_u/γ_c	$B(b \to u\ell\nu)$ (%)	R_{uc}	$\lvert V_{ub}/V_{cb}\rvert$
ACCMM	2.2±0.4	0.28±0.12±0.03	0.027±0.012	0.11±0.03±0.01
ISGW - 11% D^{**}	1.1±0.2	0.06±0.08±0.03	0.006±0.009	0.07±0.06±0.01
ISGW** - 32% D^{**}	0.9±0.2	0.25±0.10±0.02	0.022±0.009	0.16±0.03±0.02

dilepton fake rate is $n_{f\ell\ell} = N_{4S\ell} n_{f\ell}/N_{4S}$. This procedure also automatically includes the small contributions from fake-fake and cascade-fake pairs that can occur.

(iii) Cascade leptons. Leptons from $b \to c \to s\ell\nu$ decays are largely suppressed by the requirement, $p_\ell \geq 1.4$ GeV/c. We calculate the remaining background using the ACCMM and ISGW theoretical models of the $b \to c \to s\ell\nu$ spectrum. This contribution to the single lepton yield is approximately 2%. For primary-cascade pairs, the primary ($b \to c\ell\nu$) lepton can come from either the B or the $\bar{B}$ and the cascade lepton can also come from either. Hence, the cascade correction to the dilepton yields is approximately 8%.

(iv) Leptons from $B \to \psi X$. Lepton pairs from $B \to \psi X$ are removed by a mass cut as described above. However, for the single lepton yields, we must subtract an estimate of "ψ leakage", the number of leptons arising from $B \to \psi X$ decays where one of the leptons was not detected. For both the single and dilepton yields, we must add an estimate of the "ψ veto" loss, the signal lost because it appeared as combinatorial background under the ψ mass peak.

The on-$\Upsilon(4S)$ and off-$\Upsilon(4S)$ single electron and muon yields and the estimates of the fake, cascade, and $B \to \psi X$ backgrounds are given in Table IX. The corresponding dilepton yields for ee, $\mu\mu$, and $e\mu$ events are given in Table X. (All dilepton yields in this analysis include both like- and unlike-sign dileptons.) Independently of efficiencies, the numbers of ee, $\mu\mu$, and $e\mu$ dileptons should satisfy $N_{e\mu} = 2\sqrt{N_{ee}N_{\mu\mu}}$; the numbers for the two sides of this equation are, respectively, 310 ± 26 and 293 ± 27, in excellent agreement.

Since $R_{\ell\ell}$ involves the ratio of the dilepton to single lepton rates, the efficiencies for detecting single leptons enters the expression for the measured value of $R_{\ell\ell}$ [Eq. (23)]. The efficiency $\epsilon_\ell(p)$ for detecting leptons of momentum p is

$$\epsilon_\ell(p) = \epsilon_{\text{track}} a_\ell \epsilon_{\text{id}}(p), \tag{27}$$

where ϵ_{track} is the efficiency of the track-finding program for finding leptons, a_ℓ is the solid-angle acceptance of the device used for the particle identification, and $\epsilon_{\text{id}}(p)$ is the efficiency for identifying a lepton of momentum p within the solid angle a_ℓ. The track-finding efficiency is estimated to be $\epsilon_{\text{track}} = 0.99 \pm 0.01$ from a Monte Carlo calculation. The solid angles for sample A and sample B electrons and muons and the particle identification efficiencies, $\epsilon_{\text{id}}(p)$, are described in Sec. II. The overall lepton detection efficiencies, ϵ_ℓ, are given by

$$\epsilon_\ell = \sum_i \epsilon_\ell(p_i) f(p_i), \tag{28}$$

where $f(p_i)$ is the fraction of the lepton momentum spectrum in the momentum interval i and the sum runs over the range of accepted momentum, $1.4 \leq p_\ell \leq 2.5$ GeV/c. The fraction $f(p_i)$ introduces model dependence into the calculation of the efficiency. The model-dependent single-lepton efficiencies are included in Table IX. Again, the D^{**} fraction was fixed to be the 11% in the ISGW model and 32% in the ISGW** model. The consistency between the estimated efficiencies and the yields can be checked by comparing efficiency-corrected single and dilepton yields. Using the ACCMM efficiencies and including the errors in the efficiencies in the comparison, we find that the e and μ single-single lepton yields differ by 0.5 standard deviations. The χ^2 for the consistency of the efficiency-corrected ee, $\mu\mu$, and $e\mu$ yields with their average is 2.3 for 2 degrees of freedom. The consistency of the dilepton yields is actually better than this χ^2 would seem to indicate, since the errors in the efficiencies have been ignored (otherwise the calculation would be much more complicated due to correlations among the efficiency-corrected rates).

The average semileptonic branching fractions obtained from $R_{\ell\ell}$ are presented in Table XI. The numbers in the column labeled "all" in Table XI are the sums of the ee, $\mu\mu$, and $e\mu$ yields. The consistency between the measurements obtained using dileptons and the measurements obtained by fitting the lepton spectra are strong evidence that the non-$B\bar{B}$ component in $\Upsilon(4S)$ decay is not large enough to influence the measured semileptonic branching

TABLE IX. Single electron and muon yields and backgrounds. Contributions with minus signs are subtracted; as explained in the text, the ψ veto contributions are added. The cascade lepton corrections were estimated using the ACCMM model. For simplicity, the errors given for each individual contribution are the statistical and systematic errors added in quadrature. The single-lepton efficiencies calculated using the ACCMM and ISGW models are also included.

Contribution	e	μ
On $\Upsilon(4S)$	21 391±146	15 335±124
Off $\Upsilon(4S)$	−2 661± 52	−2 505± 50
$\Upsilon(4S)$	15 856±183	10 125±164
Randoms		−91± 2
Fake leptons	−320± 50	−346± 76
Cascade leptons	−380± 5	−178± 3
ψ veto	+230± 48	+168± 38
ψ leakage	−34± 18	−15± 8
Single leptons	15 352±187±62	9 662±168±83
ϵ_ℓ ACCMM	0.301±0.005	0.198±0.010
ϵ_ℓ ISGW	0.316±0.006	0.216±0.011
ϵ_ℓ ISGW**	0.286±0.005	0.180±0.009

TABLE X. Dilepton yields and backgrounds. Contributions with minus signs are subtracted; as explained in the text, the ψ veto contributions are added.

Contribution	ee	$\mu\mu$	$e\mu$
On $\Upsilon(4S)$	320±18	127±11	397±20
Off $\Upsilon(4S)$	−15± 4	−9± 3	−19± 4
$\Upsilon(4S)$	289±20	108±13	358±22
Fake leptons	−22± 8	−19± 7	−44±16
Cascade leptons	−26± 2	−6± 1	−27± 2
ψ veto	+13± 6	+2± 4	+23± 7
Dileptons	254±19±7	85±13±7	310±21±15

TABLE XI. The semileptonic B meson branching fractions obtained from the ratio of dilepton to single lepton yields. The numbers in the column labeled "all" are determined from the sums of the three lepton-pair combinations. The first error is statistical and the second is systematic.

Model	ee (%)	$\mu\mu$ (%)	All (%)
ACCMM	11.2±0.8±0.5	9.0±1.3±0.9	10.6±0.5±0.6
ISGW	10.7±0.8±0.4	8.3±1.2±0.8	9.9±0.5±0.6
ISGW**	12.0±0.9±0.5	10.0±1.5±1.0	11.5±0.6±0.6

fractions. The differences among the ACCMM, ISGW, and ISGW** models track the differences between the corresponding results from the fits to the lepton spectra. This is evidence that the most substantial difference between these models is the fraction of the lepton spectrum above $p_\ell = 1.4$ GeV/c predicted by the models.

V. TAGGED MEASUREMENTS OF b_0

A. Measuring b_0 using $\bar{B}^0 \to D^{*+}\pi^-$ tags

In the decay chain $\bar{B}^0 \to D^{*+}\pi^-$, $D^{*+} \to D^0\pi^+$, kinematic constraints can be used to reconstruct [59–61] the $\bar{B}^0$ without detecting the D^0. We interpret all oppositely charged tracks in an event as the two pions from the decays $\bar{B}^0 \to D^{*+}\pi^-$ and $D^{*+} \to D^0\pi^+$. We designate the primary π^- as the "hard" pion, with energy E_h, and the π^+ from the D^{*+} as the "soft" pion, with energy E_s. If the $\bar{B}^0$ were at rest, the momentum of the missing D^0 could be determined from four-momentum conservation alone. However, since a $\bar{B}^0$ meson produced at the $\Upsilon(4S)$ has a momentum of approximately 325 MeV/c, we have only two constraints for three unknown variables. The energy E_D of the D^0 is calculated from the conservation of energy:

$$E_D = E_{\rm beam} - E_h - E_s, \tag{29}$$

where $E_{\rm beam}$ is the beam energy. Track combinations with $E_D \leq M_D$ are rejected. The cosine of θ, the angle between the slow pion and the D^0 in the laboratory, is calculated from the D^{*+} mass:

$$\cos\theta = \frac{M_\pi^2 + M_D^2 + 2E_sE_D - M_{D^*}^2}{2p_sp_D}. \tag{30}$$

In this equation, M_π, M_D, and M_{D^*} are the masses of the charged pion, the D^0, and the D^{*+}, respectively, and p_s and p_D are the momenta of the slow pion and the D^0, respectively. Track combinations with $|\cos\theta| > 1$ cannot form a D^* and are rejected. The azimuthal angle of $\mathbf{p}_D$ about $\mathbf{p}_s$ is not determined by kinematic constraints. We choose this azimuthal angle so that the D^0 is coplanar with the hard and soft pions; this leaves a twofold ambiguity which is resolved by choosing the azimuth that gives the maximum angle between the direction of the D^0 and the direction of the hard pion. The resulting momentum of the three-particle configuration is the minimum possible, which results in the maximum possible reconstructed mass. Since the momentum of the $\bar{B}^0$ is small, this somewhat arbitrary choice does not deteriorate the resolution of the B candidate mass significantly, nor distort the shape of the background, as we show below.

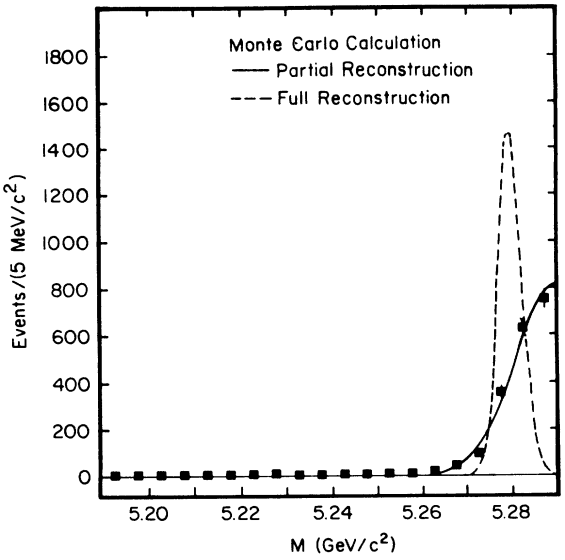

FIG. 8. Reconstructed $\bar{B}^0 \to D^{*+}\pi^-$ events from a Monte Carlo simulation. The filled squares show the mass distribution for partially reconstructed events and the solid line is the fit to this distribution described in the text; the dashed line shows the mass distribution from fully reconstructed events.

The mass of the B candidate can be written as

$$M^2 = E_{\rm beam}^2 - (p_s + p_D\cos\theta + p_h\cos\alpha)^2 - (p_D\sin\theta - p_h\sin\alpha)^2, \tag{31}$$

where α is the angle between the hard and soft pions. The mass of the $\bar{B}^0$ so determined lies between the true mass and the beam energy, a range of 10 MeV. Figure 8 shows a Monte Carlo mass distribution obtained with this procedure. The solid curve is a fit to the mass distribution using a half Gaussian centered at 5.290 GeV/c^2 with standard deviation 7.9 MeV/c^2. The dashed curve is the expected mass distribution for a full reconstruction of the $\bar{B}^0$.

To suppress the continuum under the $\Upsilon(4S)$ resonance we require that the Fox-Wolfram [37] parameter R_2 be less than 0.5 and that no track in the event have a momentum greater than half the beam energy. We require that the slow particle have dE/dx in the drift-chamber consistent with a pion. The resulting mass distribution from $\Upsilon(4S)$ data is shown in Fig. 9, where the curve is the sum of a signal which is one half of a Gaussian with mean and width fixed by the Monte Carlo calculation, a linear background, and a small background contribution from $B^- \to D^{**0}(2420)\pi^-$, $D^{**0}(2420) \to D^{*+}\pi^-$ events, estimated as described in the following paragraph. There are $N_{\rm fit} = 370\pm45\pm40$ events in the peak where the systematic error is estimated by changing the range of the fit and the order of the background polynomial. The over-

all efficiency for detecting these partially reconstructed $\bar{B}^0 \to D^{*+}\pi^-$ events is $\epsilon = 0.63 \pm 0.03$.

Because of the choice of the azimuthal angle that we introduced to complement the two kinematical constraints, it is conceivable that the signal is due to some distortion of the background. The continuum data, shown in Fig. 9, are used to demonstrate that there is no such effect from the continuum background. The difference between the solid and dashed lines in Fig. 9 represents the background due to B decays. The effect of the azimuthal angle choice on the B-decay background is investigated using Monte Carlo studies. A generic B-decay Monte Carlo simulation, excluding $\bar{B}^0 \to D^{*+}\pi^-$ decays, fails to produce a peak at the B mass. Since we are tagging neutral B mesons, our analysis will be misled only if charged B mesons can produce a peak. It is possible that this Monte Carlo calculation does not accurately describe low-multiplicity B^- decays where an unobserved soft pion might lead to a background mass peak. Possible backgrounds of this type are $B^- \to D^{*+}\pi^-\pi^-$ decays and the decay sequence $B^- \to D^{**0}(2420)\pi^-$, $D^{**0}(2420) \to D^{*+}\pi^-$. The product branching fraction for the latter decay sequence has been measured [27, 28] to be $(0.14^{+0.08}_{-0.06} \pm 0.02)\%$. A Monte Carlo simulation of the mass distribution for this decay sequence, normalized to the product branching fraction of 0.14 is illustrated in Fig. 10. The broad peak at high mass is very different from the signal in Fig. 9; it is well described by a Gaussian with area 58 events, mean 5.267 GeV/c^2, and standard deviation 38 MeV/c^2. This Gaussian was included as a background in the fit to the data in Fig. 9. The uncertainties in this product branching fraction contribute ± 10 events in quadrature to the quoted systematic uncertainty for $N_{\rm fit}$.

As a consistency check, we can obtain $B(\bar{B}^0 \to D^{*+}\pi^-)$ from $N_{\rm fit}$. However now we must also consider B^0 contamination. We study events from a Monte Carlo calculation including both charged and neutral B mesons. We do not find a mass peak in the data from which $\bar{B}^0 \to D^{*+}\pi^-$ decays have been excluded. From these data we estimate an upper limit of 64 events at 90% C.L. for the background [61] contributed by both charged and neutral B mesons. To account for these possible backgrounds, we add 40 events in quadrature to the lower systematic error in $N_{\rm fit}$, giving $N_{\rm fit} = 370 \pm 45^{+41}_{-57}$. For $B(\bar{B}^0 \to D^{*+}\pi^-)$, we then obtain

$$B(\bar{B}^0 \to D^{*+}\pi^-) = \frac{N_{\rm fit}}{2 f_0 N_{4S} \epsilon B_{D^{*+}}} = (0.46 \pm 0.06^{+0.06}_{-0.08})\%, \quad (32)$$

where N_{4S} is the number of $\Upsilon(4S)$ events in the data sample, obtained from Table I; $B_{D^{*+}}$ is the branching fraction [24]; $B(D^{*+} \to D^0\pi^+) = (55 \pm 4)\%$; and we have used $f_0 = 0.5$ (without any contribution to the systematic error). This is in good agreement with our latest result from full reconstruction [27, 28, 62] of these decays, $B(\bar{B}^0 \to D^{*+}\pi^-) = (0.47 \pm 0.12 \pm 0.06)\%$.

To determine the neutral B-meson semileptonic branching fraction with the most favorable signal to noise, we use the "signal" region $5.28 < M < 5.29$ GeV/c^2. After subtracting continuum $D^{**}\pi$ and nonresonant $D^*\pi\pi$ background contributions, there are $N_{\rm tag} = 279 \pm 29^{+26}_{-29}$ events in this interval. The systematic error is dominated by the uncertainties in the background fit. This asymmetric systematic error is due to the possible charged-B-meson contamination, which was estimated by fitting the charged-B-meson events from the Monte Carlo calculation to a linear background plus the Gaussian signal described above. We find an upper limit of 18 events at a 90% C.L. for this contribution to the background.

We define a sideband region $5.20 < M < 5.27$ GeV/c^2 which is used to estimate the continuum and B-meson background in the signal region. We search for leptons with momentum between 1.4 and 2.4 GeV/c in both regions. The average of the efficiencies for detect-

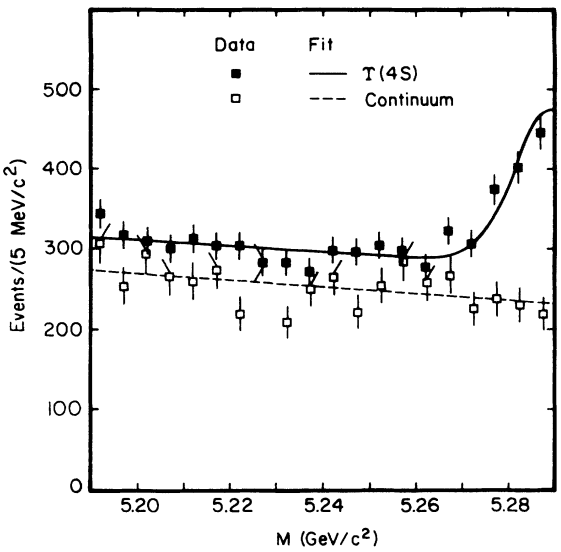

FIG. 9. The mass distribution from partially reconstructed $\bar{B}^0 \to D^{*+}\pi^-$ candidates. Filled squares are $\Upsilon(4S)$ data and open squares are continuum data scaled by the luminosity factor $f_{\mathcal{L}} = 2.08$. The solid and dashed lines are fits described in the text to the $\Upsilon(4S)$ and continuum data, respectively.

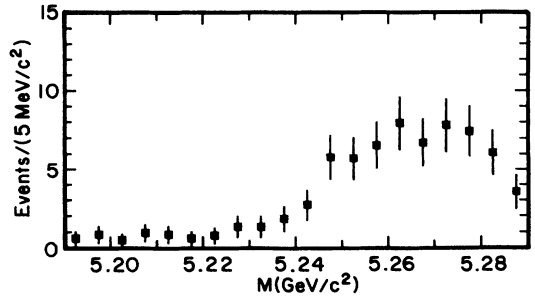

FIG. 10. The mass distribution for partially reconstructed $\bar{B}^0 \to D^{*+}\pi^-$ candidates, obtained from a Monte Carlo simulation of $B^- \to D^{**0}(2420)\pi^-$, $D^{**0}(2420) \to D^{*+}\pi^-$ events. The number of events is normalized to a product branching fraction of 0.14%.

TABLE XII. Lepton yields and backgrounds for events tagged with $\bar{B}^0 \to D^{*+}\pi^-$ and $\bar{B}^0 \to D^{*+}\ell^-\bar{\nu}$ decays.

	$\bar{B}^0 \to D^{*+}\pi^-$ tag		$\bar{B}^0 \to D^{*+}\ell^-\bar{\nu}$ tag	
	Right sign	Wrong sign	Right sign	Wrong sign
Observed leptons	23 ±4.8	8 ±2.8	7 ±2.6	0 ±1.2
Combinatorial background	6.4±1.0	5.0±0.8	1.48±0.53	0.27±0.11
Fake leptons	0.2±0.0	0.4±0.0	0.08±0.03	0.07±0.03
Cascade - same B	1.6±0.1			
Cascade - other B	0.1±0.0	0.3±0.1	0.02±0.00	0.09±0.03
Net lepton yield	14.7±4.9	2.3±2.9	5.4 ±2.7	-0.4 ±1.2
Total lepton yield	17.0 ± 5.7		5.0 ± 3.0	

ing electrons and muons between 1.4 and 2.4 GeV/c is $\epsilon_\ell = 0.28 \pm 0.01$. The lepton efficiency includes the fraction of the lepton spectrum above 1.4 GeV/c, estimated using the ISGW model [46]; the systematic error is dominated by the uncertainty in this fraction. Leptons with charge opposite to that of the hard pion in the tagged $\bar{B}^0 \to D^{*+}\pi^-$ decay are called right-sign leptons, while leptons with the same charge as the hard pion (arising from mixed $B^0\bar{B}^0$ events) are called wrong-sign leptons. In the right-sign sample we find 12 electrons and 11 muons; in the wrong-sign sample we find 5 electrons and 3 muons. The lepton yields for tagged events and their backgrounds are given in Table XII. For right-sign leptons, the sideband region yields a background estimate of 6.4 ± 1.0 leptons of which 2.8 ± 0.5 are due to continuum processes.

To estimate the background due to fake leptons we take all events in the signal region and search for any track in the correct momentum range not positively identified as a lepton. We multiply the number of such tracks by the average fake probability to determine the fake contribution [61]. In addition there are two other sources of background leptons.

(i) A cascade lepton from the semileptonic decay of the undetected D^0 resulting from $\bar{B}^0 \to D^{*+}\pi^-$ decay; this yields only right-sign leptons.

(ii) A cascade lepton from the semileptonic decay of a D meson resulting from the decay of the other B meson; this yields right-sign leptons in mixed events and wrong-sign leptons in unmixed events.

These backgrounds are estimated [61] using measured semileptonic D^0 branching fractions. Both backgrounds are small because little of the cascade lepton spectrum is above 1.4 GeV/c, even in the first case where the D^0 is relatively hard. The background from the second case is further reduced because mixing is required. For estimating this background we use the value of r given in Eq. (15).

TABLE XIII. Tagged measurements of branching fractions for semileptonic decay of neutral B mesons.

Tag	b_{0r} (%)	b_0 (%)
$\bar{B}^0 \to D^{*+}\pi^-$	9.4±3.3±1.0	10.9±3.8±1.2
$\bar{B}^0 \to D^{*+}\ell^-\bar{\nu}$	8.8±4.5±0.7	8.2±5.0±0.6
Average	9.2±2.7±0.9	9.9±3.0±0.9

The net yields of right- and wrong-sign leptons are included in Table XII. The semileptonic branching fraction b_{0r}, calculated from the number of right-sign leptons n_{0r} using

$$b_{0r} = \frac{n_{0r}}{2\epsilon_\ell N_{\rm tag}} \tag{33}$$

is given in Table XIII. We can eliminate the effect of mixing by including both right-sign and wrong-sign leptons. The total lepton yield is included in Table XII, and the corresponding value of b_0 given in Table XIII; it is consistent with the average branching fraction $\langle b \rangle$ measured using the untagged semileptonic spectrum.

B. Measuring b_0 using $\bar{B}^0 \to D^{*+}\ell^-\bar{\nu}$ tags

The reconstruction of neutral B mesons using the decay $\bar{B}^0 \to D^{*+}\ell^-\bar{\nu}$ is extensively described elsewhere [56, 63, 64]. Briefly, we reconstruct the decay $\bar{B}^0 \to D^{*+}\ell^-\bar{\nu}$ using a missing-mass technique. Because B mesons are produced nearly at rest at the $\Upsilon(4S)$ resonance one can use the fact that $E_B = E_{\rm beam}$ and $p_B = 325$ MeV/$c \approx 0$ to write the missing mass squared as

$$MM^2 = [E_{\rm beam} - (E_{D^*} + E_\ell)]^2 - (\mathbf{p}_{D^*} + \mathbf{p}_\ell)^2. \tag{34}$$

The MM^2 distribution for $D^{*+}\ell^-$ is shown in Fig. 11.

The prominent peak at $MM^2 \approx 0$ is evidence for the decay $\bar{B}^0 \to D^{*+}\ell^-\bar{\nu}$. The width of the MM^2 distribution [full width at half maximum (FWHM) = 0.8 (GeV/c^2)^2] arises from neglecting the momentum of the B meson. We select a sample of tagged neutral B mesons by requiring a 3σ cut on the MM^2 distribution [$-1 < MM^2 < 1$ (GeV/c^2)^2].

From the fit to the missing-mass-squared distribution we obtain the numbers of candidate and background events shown in Table XIV. We find $N_{\rm tag} = 109 \pm 13 \pm 7$ $D^{*+}\ell^-\bar{\nu}$ events, $N_{\rm other} = 28.5 \pm 10$ events due to other B-meson decays, and $N_{\rm cont} = 6.2 \pm 3.0$ continuum events. The systematic uncertainty in $N_{\rm tag}$ is obtained by fitting the MM^2 distribution with and without a D^{**} component.

In order to measure the inclusive semileptonic branching fraction we search for a second lepton with momen-

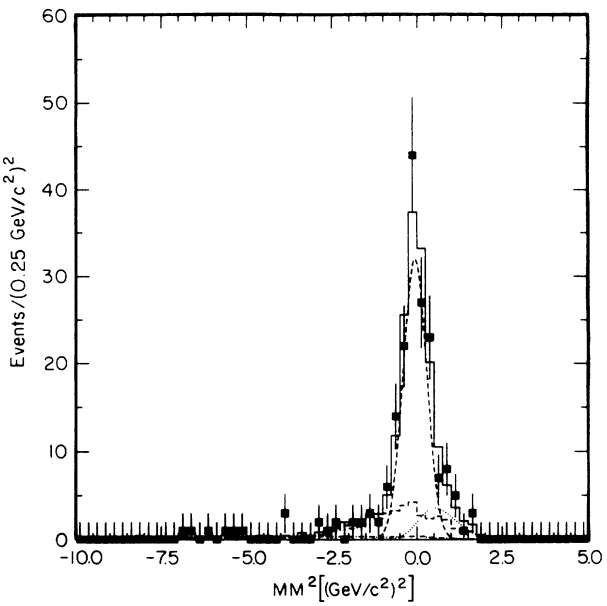

FIG. 11. Missing-mass-squared distribution for $\bar{B}^0 \to D^{*+}\ell^-\bar{\nu}$. The filled squares are the data points, the solid histogram is the result of the fit with a Gaussian for the signal and a background. The background due to mixing and cascades is the dot-dashed histogram, the background due to fake D^*'s is the dashed histogram, and the background due to excited D^*'s is the dotted line.

tum between 1.4 and 2.4 GeV/c in the event. The average efficiency for detecting a lepton with momentum between 1.4 and 2.4 GeV/c, calculated using the ISGW [46] model is $\epsilon_\ell = 0.28 \pm 0.01$. We find 7 right-sign ($D^{*+}\ell^-\ell^+$) events and 0 wrong-sign ($D^{*+}\ell^-\ell^-$) events. Since we did not find any wrong-sign events, we estimate the error in this number from our estimate of the number of expected events using $N_{\rm tag}$, ϵ_ℓ, $\langle b\rangle$ [from Eq. (19)], and r. We find that we expect 1 signal event and 0.4 background events, so we assign the error ± 1.2 to the number of wrong-sign tagged leptons. Three of the four kinds of background present in the $\bar{B}^0 \to D^{*+}\pi^-$ tagged sample are also present in this tagged sample; background from the semileptonic decay of the tagging D is not present because the tagging D is reconstructed from decays to hadronic modes. The numbers of tagged leptons and the estimated backgrounds are included in Table XII.

The contribution to the combinatorial background due to B-meson decays other than $\bar{B}^0 \to D^{*+}\ell^-\bar{\nu}$ is estimated from $N_{\rm other}$, assuming that they are all from neutral B-meson decays. The background due to semileptonic decay of the other B meson in the event is twice the product of $N_{\rm other}$, $\langle b\rangle$, and ϵ_ℓ. There is also a small contribution due to the semileptonic decay of charm daughters from the decay of the other B meson. The total of these estimated contaminations is 1.7 ± 0.5 events. The contamination for right-sign events is $1/(1+r)$ times this number and the contamination for wrong-sign events is $r/(1+r)$ times this number. These backgrounds are included in Table XII.

The continuum contribution to the combinatorial background is estimated by using the continuum background, $N_{\rm cont}$, in our tagged sample, the measured branching fraction [13], $B(e^+e^- \to q\bar{q} \to X\ell^-\bar{\nu}) = 0.080 \pm 0.009$, an average lepton efficiency, 0.52 ± 0.02, and the fraction of leptons from charm above 1.4 GeV/c, 0.02 ± 0.005. By multiplying these numbers we obtain 0.005 ± 0.003 events, so the continuum contribution is negligible.

To estimate the background due to fake leptons we take all events in the interval $-1 < MM^2 < 1$ (GeV/c^2)^2 and search for any track in the correct momentum range not positively identified as a lepton. We find 7 right-sign tracks and 6 wrong-sign tracks. Weighting these tracks with the momentum-dependent fake rate yields the numbers given in Table XII.

The final background arises from the cascade decay of a D from the other B in the event. This can be either right or wrong sign depending on whether or not the B mixes before decay. Our estimates of these backgrounds are also included in Table XII.

The net lepton yields for right- and wrong-sign leptons are given in Table XII and the corresponding branching fractions b_{0r} and b_0 are given in Table XIII. The value of b_0 obtained with this tag is consistent with our measurement of $\langle b\rangle$, and these values of b_{0r} and b_0 are consistent with those obtained from the $\bar{B}^0 \to D^{*+}\pi^-$ partial reconstruction tag.

TABLE XIV. $\bar{B}^0 \to D^{*+}\ell^-\bar{\nu}$ signal and backgrounds for $|MM|^2 < 1$ GeV^2.

Source	Events
Signal events – $N_{\rm tag}$	109±13
Continuum events – $N_{\rm cont}$	6.2±3.0
Fake leptons	2.2±0.3
Fake D^{*+}'s	8.3±0.4
Mixed events and cascades	1.1±0.4
$D^{**}\pi$ and nonresonant $D^*\pi\pi$	16.9±10
Total – $N_{\rm other}$	28.5±10

C. Average of the two measurements of b_0

The results obtained with the two tagging methods are in good agreement. Since they are statistically independent we combine them; the averages are included in Table XIII. The average value of b_0 is consistent with $\langle b\rangle$ [Eq. (19)]; their ratio is

$$\frac{\langle b\rangle}{b_0} = 1.09 \pm 0.33 \pm 0.04. \tag{35}$$

Since this ratio is 1 within the experimental error, there is no evidence for a difference between the branching fractions b_0 and b_-. The value of μ [Eq. (4)] derived from this ratio is

$$\mu = \frac{f_- b_-}{f_0 b_0} = (1+\phi)\frac{\langle b\rangle}{b_0} - 1 = 1.18 \pm 0.66 \pm 0.08, \tag{36}$$

compared to $\mu = 0.90 \pm 0.17$ from the average of the

ARGUS and CLEO measurements of this ratio [Eq. (5)]. More precise measurements of the ratio of b_- to b_0 will require large tagged samples of both charged and neutral B mesons from $\Upsilon(4S)$ decay.

D. Correcting b_{0r} for mixing to obtain b_0

Instead of using both right-sign and wrong-sign tagged leptons to measure b_0, it is possible to obtain a modest improvement in the statistical error for b_0 by using the measured value of ρ [Eq. (12)] the ratio of like-sign to opposite-sign dileptons at the $\Upsilon(4S)$ to correct b_{0r} for mixing. However, this procedure requires some knowledge of f_0 and f_-, as well as a measurement of $\langle b \rangle$. Using Eq. (13) giving r in terms of ρ and λ, Eq. (6) defining $\langle b \rangle$, Eq. (16) relating b_0 to b_{0r} and r, and Eq. (3) defining λ, we derive a quadratic equation for b_0 in terms of b_{0r} by eliminating b_-:

$$f_0[f_- - \rho f_0]b_0^2 + f_0[2\rho\langle b \rangle - b_{0r}(1+\rho)f_-]b_0 - \rho\langle b^2 \rangle = 0. \tag{37}$$

To calculate b_0 we use the average value of b_{0r} from Table XIII, $\langle b \rangle$ from Eq. (19), and the average of the ARGUS and CLEO values for ρ from Eq. (14). As noted in Sec. II, we do not have any direct measurements for f_0 and f_-. However, we use the theoretical result, $\phi = 1.00 \pm 0.05$, [Eq. (10)] and we assume that f, the fraction of non-$B\bar{B}$ decays is negligible. We find

$$b_0 = B(\bar{B}^0 \to X^+ \ell^- \bar{\nu}) = (10.8 \pm 2.3 \pm 0.8)\%, \tag{38}$$

where the statistical and systematic errors include the uncertainties in b_{0r}, $\langle b \rangle$, and ρ. The systematic error is quite insensitive to the uncertainty in ϕ because $db_0/d\phi = 0.007$. Although there is modest improvement in the dominant statistical error in the measurement of b_0 using this procedure, we prefer to quote the average of the two direct measurements using both wrong- and right-sign leptons because the direct result is less dependent on other measurements.

VI. CONCLUSIONS

We have measured the average B-meson semileptonic branching fraction by fitting the lepton spectra from B decay to the distributions predicted by the ACCMM [43] modified free-quark model and the ISGW [46] form-factor model. We obtain $B(\bar{B} \to X\ell^-\bar{\nu}) = (10.5 \pm 0.2 \pm 0.4)\%$ using the ACCMM model and $B(\bar{B} \to X\ell^-\bar{\nu}) = (9.9 \pm 0.1 \pm 0.4)\%$ using the ISGW model. However, the fit to the ISGW data has an uncomfortably large χ^2, so we quote the ISGW result only for comparison with other experiments that have used this model.

We obtain a substantially better fit (the χ^2 of the fit decreases by 25) using the ISGW model if the $D^{**}\ell^-\bar{\nu}$ contribution is allowed to rise from the 11% predicted by the ISGW model to 32%. The resulting branching fraction for the ISGW** model is $B(\bar{B} \to X\ell^-\bar{\nu}) = (11.2 \pm 0.3 \pm 0.4)\%$; this increase in the $b \to q\ell\nu$ branching fraction is at the expense of the branching fraction for leptons from cascade $b \to c \to s\ell\nu$ decays. Although we are not certain that the shape of the lepton spectrum from $\bar{B} \to D^{**}\ell^-\bar{\nu}$ decays in the ISGW model accurately represents the contribution to the low-momentum lepton spectrum due to high-mass charm states, the very large decrease in χ^2 shows that the resulting spectrum represents the experimental data much better than the spectrum of the original ISGW model. Our best estimate of the semileptonic branching fraction of B mesons is the average of this ISGW** result with that of the ACCMM model:

$$B(\bar{B} \to X\ell^-\bar{\nu}) = (10.8 \pm 0.2 \pm 0.4 \pm 0.4)\%, \tag{39}$$

where the errors are statistical, systematic uncertainties in the measurement, and systematic uncertainties associated with the theoretical models, respectively.

The average semileptonic branching fraction was also measured using dilepton events to eliminate the uncertainties due to possible non-$B\bar{B}$ decays of the $\Upsilon(4S)$. Using this technique we obtain, $B(\bar{B} \to X\ell^-\bar{\nu}) = (10.6 \pm 0.5 \pm 0.6)\%$ using the ACCMM model, $B(\bar{B} \to X\ell^-\bar{\nu}) = (9.9 \pm 0.5 \pm 0.6)\%$ using the ISGW model, and $B(\bar{B} \to X\ell^-\bar{\nu}) = (11.5 \pm 0.6 \pm 0.6)\%$ using the ISGW** model. The excellent agreement between these results and the corresponding results from the fits to the lepton spectra shows that non-$B\bar{B}$ decays of the $\Upsilon(4S)$ are small enough to be safely ignored in the measurements of the semileptonic branching fractions reported here.

We have also measured the B^0 semileptonic branching fraction by tagging a $\bar{B}^0$ from the $\Upsilon(4S)$ using $\bar{B}^0 \to D^{*+}\pi^-$ and $\bar{B}^0 \to D^{*+}\ell^-\bar{\nu}$ decays, and counting the number of leptons from the B^0 decay. From these tagged measurements, we obtain $(9.9 \pm 3.0 \pm 0.9)\%$ which, together with the result for the average semileptonic branching fraction, is additional evidence that the charged and neutral B mesons have similar semileptonic branching fractions and lifetimes.

Taking all experimental and model uncertainties into account, our measurements of the semileptonic branching fraction for B-meson decay are substantially lower than the 12% that can be gracefully accommodated by typical pure spectator models of B decay [10], but are well within the range predicted by more recent theoretical estimates including nonspectator diagrams [16].

ACKNOWLEDGMENTS

We thank J.C. Gabriel, W.J. Marciano, G.P. Lepage, and T.M. Yan for useful discussions. We gratefully acknowledge the effort and success of the CESR staff in producing the luminosity for this experiment. P.S.D. thanks the PYI program of the NSF, and R.P. thanks the A.P. Sloan Foundation for support. This work was supported by the National Science Foundation and the U.S. Dept. of Energy under Contract Nos. DE-(AC02(76ER(01428, 03064, 01545), 78ER05001, 83ER40103), and FG05-86ER40272). The supercomputing resources of the Cornell Theory Center were used in this research.

[1] In this paper the term "lepton" and the symbol "ℓ" always refer to an e or a μ, never to a τ. The term "semileptonic branching fraction" and expressions such as $B(\bar{B} \to X\ell^-\bar{\nu})$ and $B(b \to q\ell\nu)$ always refer to the branching fraction for decay to e or μ or the average of the two; they never refer to the sum of the branching fractions for decay to e and μ. The results quoted in the abstract and text are always the average of the e and μ results; individual e and μ results are quoted only in the tables.

[2] H. Fritzsch and P. Minkowski, Phys. Rep. **73**, 6 (1981).

[3] R. Schindler, in *High Energy Electron-Positron Physics,* edited by A. Ali and P. Söding (World Scientific, Singapore, 1988), p. 234.

[4] R. Rückl, Habilitationsschrift, Universität München, 1984.

[5] A.J. Buras, J.-M. Gerard, and R. Rückl, Nucl. Phys. **B268**, 16 (1986).

[6] M.A. Shifman, in *Lepton and Photon Interactions,* Proceedings of the 1987 International Symposium on Lepton and Photon Interactions at High Energies, Hamburg, West Germany, 1987, edited by R. Rückl and W. Bartel [Nucl. Phys. B (Proc. Suppl.) **3**, 289 (1988)].

[7] I.I. Bigi, in *Proceedings of the International Symposium on Heavy Quark Physics,* Cornell University, Ithaca, New York, 1989, edited by P.S. Drell and D.L. Rubin, AIP Conf. Proc. No. 196 (AIP, New York, 1989), p. 18.

[8] I.I. Bigi and B. Stech, in *Proceedings of the Workshop on High Sensitivity Beauty Physics,* Batavia, Illinois, 1987, edited by A.J. Slaughter, N. Lockyer, and M. Schmidt (Fermilab, Batavia, IL, 1988).

[9] M. Kobayashi and T. Maskawa, Prog. Theor. Phys. **49**, 652 (1973).

[10] A. Khodjamirian, S. Rudaz, and M.B. Voloshin, Phys. Lett. B **242**, 489 (1990).

[11] Crystal Ball Collaboration, K. Wachs *et al.*, Z. Phys. C **42**, 33 (1989).

[12] CLEO Collaboration, S. Behrends *et al.*, Phys. Rev. Lett. **59**, 407 (1987).

[13] R. Kowalewski, Ph.D. thesis, Cornell University, 1988. This thesis contains the results of a reanalysis of the same data sample that was used in Ref. [12]. The momentum-resolution and particle-identification efficiencies were substantially improved between the two analyses. The semileptonic branching fractions obtained in the newer analysis are smaller than those obtained in the previous analysis.

[14] ARGUS Collaboration, H. Albrecht *et al.*, Phys. Lett. B **249**, 359 (1990).

[15] CUSB Collaboration, C. Yanagisawa *et al.*, Phys. Rev. Lett. **66**, 2436 (1991).

[16] G. Altarelli and S. Petrarca, Phys. Rev. Lett. B **261**, 303 (1991).

[17] In this paper any mention of particles and their decays also implies the corresponding antiparticles and their decays.

[18] This assumption has been verified for D meson semileptonic decay, cf. R.H. Schindler, in *Proceedings of the XXIVth International Conference on High Energy Physics,* Munich, West Germany, 1988, edited by R. Kotthaus and J. Kuhn (Springer-Verlag, Berlin, 1989).

[19] ARGUS Collaboration, H. Albrecht *et al.*, Phys. Lett. B **192**, 245 (1987). We use an updated result reported by H. Schröder, in *Physics in Collision 10,* Proceedings of the International Conference, Durham, NC, 1990, edited by A. Goshaw and L. Montanet (World Scientific, Singapore, 1990).

[20] CLEO Collaboration, M. Artuso *et al.*, Phys. Rev. Lett. **62**, 2233 (1989).

[21] ARGUS Collaboration, H. Albrecht *et al.*, Phys. Lett. B **232**, 554 (1989).

[22] CLEO Collaboration, R. Fulton *et al.*, Phys. Rev. D **43**, 641 (1991).

[23] G. Crawford, Ph.D. thesis, Cornell University, 1991.

[24] Particle Data Group, J.J. Hernández *et al.*, Phys. Lett. B **239**, 1 (1990).

[25] CLEO Collaboration, Internal Report No. CBX92-09 (unpublished).

[26] ARGUS Collaboration, H. Albrecht *et al.*, Z. Phys. C **48**, 543 (1990).

[27] J.D. Lewis, Ph.D. thesis, Cornell University, 1990.

[28] CLEO Collaboration, D. Bortoletto *et al.,* Phys. Rev. D **45**, 21 (1992).

[29] D. Atwood and W.J. Marciano, Phys. Rev. D **41**, 1736 (1990).

[30] G.P. Lepage, Phys. Rev. D **42**, 3251 (1990).

[31] N. Byers and E. Eichten, Phys. Rev. D **42**, 3885 (1990).

[32] CLEO Collaboration, D. Andrews *et al.*, Nucl. Instrum. Methods **211**, 47 (1983).

[33] CLEO Collaboration, T. Bowcock *et al.*, Phys. Rev. D **41**, 805 (1990).

[34] CLEO Collaboration, C. Bebek *et al.*, Phys. Rev. D **36**, 690 (1987).

[35] D.G. Cassel *et al.*, Nucl. Instrum. Methods. **A252**, 325 (1986).

[36] CLEO Collaboration, S. Behrends *et al.*, Phys. Rev. D **31**, 2161 (1985).

[37] G. Fox and S. Wolfram, Phys. Rev. Lett. **41**, 1581 (1978). We define $R_1 = H_1/H_0$ and $R_2 = H_2/H_0$.

[38] CLEO Collaboration, M.S. Alam *et al.*, Phys. Rev. D **40**, 712 (1989).

[39] M. Worris, Ph.D. thesis, Cornell University, 1991.

[40] CLEO Collaboration, R. Fulton *et al.*, Phys. Rev. Lett. **64**, 16 (1990).

[41] CLEO Collaboration,Y. Kubota in the *Proceedings of the International Symposium on Heavy Quark Physics,* Cornell University, Ithaca, New York, 1989, edited by P.S. Drell and D.L. Rubin, AIP Conf. Proc. No. 196 (AIP, New York, 1989), p. 142.

[42] The $B \to X\tau\nu$ fraction is estimated from the semileptonic branching fraction of about 10% that we measure, the $\tau \to X\ell\nu$ branching fraction, and the phase-space correction due to the mass of the τ.

[43] G. Altarelli, N. Cabibbo, G. Corbò, L. Maiani, and G. Martinelli, Nucl. Phys. **B208**, 365 (1982).

[44] M. Jeżabek *et al.*, Nucl. Phys. **B320**, 20 (1989). The QCD corrections to the lepton momentum spectrum have little effect on the spectral shape but are a significant correction to the integrated width.

[45] DELCO Collaboration, W. Bacino *et al.*, Phys. Rev. Lett. **43**, 1073 (1979).

[46] N. Isgur, D. Scora, B. Grinstein, and M. B. Wise, Phys. Rev. D **39**, 799 (1989). In previous CLEO analyses, an earlier version of this model, B. Grinstein, M. B. Wise, and N. Isgur, Phys. Rev. Lett. **56**, 298 (1986), was used.

[47] CLEO Collaboration, D. Bortoletto *et al.*, Phys. Rev. D **35**, 19 (1987).

[48] We average the results of the two models with equal

weights, since the same data are used for the fits to each model and the experimental systematic errors are common to the two models.

[49] An earlier version of the ISGW model was used in [13].

[50] In the fit, we fix the D^*/D ratio to be the value 2.3 obtained from the ISGW model, which also agrees with our exclusive measurement described in Ref. [22]. The D^*/D ratio must be constrained in order to obtain reasonable fits; there is not enough difference between the D^* and D lepton spectra to determine this ratio from the inclusive lepton spectrum.

[51] CLEO Collaboration, M.S. Alam *et al.*, Phys. Rev. Lett. **59**, 22 (1987); G. Crawford *et al.*, Phys. Rev. D **45**, 752 (1992).

[52] The ISGW model predicts the rates for $B \to D\ell\nu$, $D^*\ell\nu$, and $D^{**}\ell\nu$. The value $\gamma_c = 41$ ps^{-1} represents the sum of these three rates. Among the calculations by J.G. Körner and G.A. Schuler, Z. Phys. C **38**, 511 (1988), M. Wirbel, B. Stech, and M. Bauer, *ibid.* **29**, 637 (1985), and T. Altomari and L. Wolfenstein, Phys. Rev. D **37**, 681 (1988), whose approaches are similar to that of ISGW, the coefficient varies by about 10%. However, since ISGW estimate an uncertainty of 20% in their calculation, we use this number for the uncertainty in γ_c.

[53] The systematic error assumes a 20% uncertainty in γ_c from the ACCMM model.

[54] We have not attempted to include an estimate of the systematic error due to possible differences between the lifetimes of charged and neutral B mesons or for the fact that the measured lifetimes are for unknown mixtures (possibly different in different experiments) of B^0, B^-, B_s, and b flavored baryons.

[55] ALEPH Collaboration, D. Decamp *et al.*, Phys. Lett. B **257**, 492 (1991).

[56] CLEO Collaboration, D. Bortoletto, Phys. Rev. Lett. **63**, 1667 (1989). In this paper $|V_{cb}| = 0.039 \pm 0.004$.

[57] Another similar ratio, $\alpha = 4N_{4S}N_{\ell\ell}/(gN_\ell^2) = (f_0 b_0^2 + f_- b_-^2)/(f_0 b_0 + f_- b_-)^2 = \langle b^2\rangle/\langle b\rangle^2$, is sensitive to f, but not to b, ϕ, and β in the same limit; it was used in Ref. [25] to determine the upper limit for f. In general, ratios of powers of $\langle b^2\rangle$ and $\langle b\rangle$ are very insensitive to combinations of b_0 and b_- or f_0 and f_- that appear to the same power in the numerator and denominator, as long as ϕ and β are near 1.

[58] The yields used in this analysis are somewhat larger than those reported in Ref. [25] to determine an upper limit for f. The selection criteria imposed in Ref. [25] are more stringent than those used here, in order to more closely match the criteria used in Ref. [40], the CLEO measurement of $b \to u\ell\nu$.

[59] CLEO Collaboration, R. Giles *et al.*, Phys. Rev. D **30**, 2279 (1984).

[60] ARGUS Collaboration, H. Albrecht *et al.*, Phys. Lett. B **182**, 95 (1986).

[61] W.-C. Li, Ph.D. thesis, State University of New York at Albany, 1990.

[62] The result quoted here has been corrected for the PDG values [24] of the D^{*+} and D^0 branching ratios.

[63] ARGUS Collaboration, H. Albrecht *et al.*, Phys. Lett. B **197**, 452 (1987).

[64] D. Bortoletto, Ph.D. thesis, Syracuse University, 1989.